

A Cartesian Cut Cell Method for Rarefied Flow Simulations around Moving Obstacles

G. Dechiste¹, L. Mieussens²

¹UMR 1013, CNRS, INRIA
UMR 1013, CNRS, INRIA
(Guillaume.Dechriste@math.u-bordeaux1.fr)

²UMR 1013, CNRS, INRIA
UMR 1013, CNRS, INRIA
UMR 1013, CNRS, INRIA
UMR 1013, CNRS, INRIA
(Luc.Mieussens@math.u-bordeaux1.fr)

Abstract

For accurate simulations of rarefied gas flows around moving obstacles, we propose a cut cell method on Cartesian grids: it allows exact conservation and accurate treatment of boundary conditions. Our approach is designed to treat Cartesian cells and various kind of cut cells by the same algorithm, with no need to identify the specific shape of each cut cell. This makes the implementation quite simple, and allows a direct extension to 3D problems. Such simulations are also made possible by using an adaptive mesh refinement technique and a hybrid parallel implementation. This is illustrated by several test cases, including a 3D unsteady simulation of the Crookes radiometer.

~~arXiv:1508.01234v1 [physics.flu-dyn]~~

1 Introduction

In this paper, we propose a Cartesian cut cell method for the simulation of rarefied gas flows around moving obstacles. The method is based on a Cartesian grid and a cut cell approach. The cut cells are defined by the intersection of the grid and the obstacle. The method is designed to be simple and efficient. It allows the simulation of rarefied gas flows around moving obstacles. The method is based on a Cartesian grid and a cut cell approach. The cut cells are defined by the intersection of the grid and the obstacle. The method is designed to be simple and efficient. It allows the simulation of rarefied gas flows around moving obstacles.

As a result, we obtain a simple and efficient method for the simulation of rarefied gas flows around moving obstacles.

(M. 73) ~~...~~
f. 100r
f. 100v
f. 101r
f. 101v
f. 102r
f. 102v
f. 103r
f. 103v
f. 104r
f. 104v
f. 105r
f. 105v
f. 106r
f. 106v
f. 107r
f. 107v
f. 108r
f. 108v
f. 109r
f. 109v
f. 110r
f. 110v
f. 111r
f. 111v
f. 112r
f. 112v
f. 113r
f. 113v
f. 114r
f. 114v
f. 115r
f. 115v
f. 116r
f. 116v
f. 117r
f. 117v
f. 118r
f. 118v
f. 119r
f. 119v
f. 120r
f. 120v
f. 121r
f. 121v
f. 122r
f. 122v
f. 123r
f. 123v
f. 124r
f. 124v
f. 125r
f. 125v
f. 126r
f. 126v
f. 127r
f. 127v
f. 128r
f. 128v
f. 129r
f. 129v
f. 130r
f. 130v
f. 131r
f. 131v
f. 132r
f. 132v
f. 133r
f. 133v
f. 134r
f. 134v
f. 135r
f. 135v
f. 136r
f. 136v
f. 137r
f. 137v
f. 138r
f. 138v
f. 139r
f. 139v
f. 140r
f. 140v
f. 141r
f. 141v
f. 142r
f. 142v
f. 143r
f. 143v
f. 144r
f. 144v
f. 145r
f. 145v
f. 146r
f. 146v
f. 147r
f. 147v
f. 148r
f. 148v
f. 149r
f. 149v
f. 150r
f. 150v
f. 151r
f. 151v
f. 152r
f. 152v
f. 153r
f. 153v
f. 154r
f. 154v
f. 155r
f. 155v
f. 156r
f. 156v
f. 157r
f. 157v
f. 158r
f. 158v
f. 159r
f. 159v
f. 160r
f. 160v
f. 161r
f. 161v
f. 162r
f. 162v
f. 163r
f. 163v
f. 164r
f. 164v
f. 165r
f. 165v
f. 166r
f. 166v
f. 167r
f. 167v
f. 168r
f. 168v
f. 169r
f. 169v
f. 170r
f. 170v
f. 171r
f. 171v
f. 172r
f. 172v
f. 173r
f. 173v
f. 174r
f. 174v
f. 175r
f. 175v
f. 176r
f. 176v
f. 177r
f. 177v
f. 178r
f. 178v
f. 179r
f. 179v
f. 180r
f. 180v
f. 181r
f. 181v
f. 182r
f. 182v
f. 183r
f. 183v
f. 184r
f. 184v
f. 185r
f. 185v
f. 186r
f. 186v
f. 187r
f. 187v
f. 188r
f. 188v
f. 189r
f. 189v
f. 190r
f. 190v
f. 191r
f. 191v
f. 192r
f. 192v
f. 193r
f. 193v
f. 194r
f. 194v
f. 195r
f. 195v
f. 196r
f. 196v
f. 197r
f. 197v
f. 198r
f. 198v
f. 199r
f. 199v
f. 200r
f. 200v

...

...

The Boltzmann equation is a partial differential equation that describes the evolution of the distribution function $F(t, \vec{x}, \vec{v})$ in phase space. It is derived from the Liouville equation by taking the first moment and assuming a Maxwellian distribution for the background gas. The equation is written as:

$$\frac{\partial F}{\partial t} + \vec{v} \cdot \nabla F = Q(F).$$

where $F(t, \vec{x}, \vec{v})$ is the distribution function, $\vec{x} \in \mathbb{R}^3$ is the position vector, $\vec{v} \in \mathbb{R}^3$ is the velocity vector, and $Q(F)$ is the collision operator. The collision operator represents the change in the distribution function due to collisions between particles.

2 Rarefied gas dynamics

2.1 Boltzmann equation

The Boltzmann equation is

$$\frac{\partial F}{\partial t} + \vec{v} \cdot \nabla F = Q(F). \quad (1)$$

where $F(t, \vec{x}, \vec{v})$ is the distribution function, $\vec{x} \in \mathbb{R}^3$ is the position vector, $\vec{v} \in \mathbb{R}^3$ is the velocity vector, and $Q(F)$ is the collision operator. The collision operator represents the change in the distribution function due to collisions between particles.

$$\frac{\partial}{\partial t} \int_V F dV + \int_{\partial V} (\vec{v} - \vec{w}) \cdot \vec{n} F dS = \int_V Q(F) dV, \quad (2)$$

where $\partial V(t)$ is the boundary of the volume $V(t)$, $\vec{w}(t, \vec{x})$ is the velocity of the boundary, and $\vec{n}(t, \vec{x})$ is the normal vector to the boundary.

The macroscopic quantities are defined as:

Definition 3.1

$$\begin{aligned} \begin{bmatrix} \rho \\ \rho \vec{u} \\ E \end{bmatrix} &= \int_{\mathbb{R}^3} \begin{bmatrix} 1 \\ \|\vec{v}\| \\ \frac{1}{2}\|\vec{v}\|^2 \end{bmatrix} F(t, \vec{x}, \vec{v}) \, dv_x dv_y dv_z, \\ \vec{\Sigma} &= \int_{\mathbb{R}^3} (\vec{v} - \vec{u}) \otimes (\vec{v} - \vec{u}) F(t, \vec{x}, \vec{v}) \, dv_x dv_y dv_z, \\ \vec{q} &= \int_{\mathbb{R}^3} \frac{1}{2}(\vec{v} - \vec{u}) \|\vec{v} - \vec{u}\|^2 F(t, \vec{x}, \vec{v}) \, dv_x dv_y dv_z, \end{aligned} \tag{3}$$

where

$$\begin{aligned} \|\vec{v}\|^2 &= v_x^2 + v_y^2 + v_z^2, \quad T \text{ is the temperature,} \\ E &= \frac{1}{2}\rho\|\vec{u}\|^2 + \frac{3}{2}\rho RT, \quad R \text{ is the gas constant.} \end{aligned}$$

where

is the mass flux

is the momentum flux

is the energy flux

is the stress tensor

is the heat flux

$$P = \rho RT.$$

$$\mathcal{M}[\rho, \vec{u}, T](\vec{v}) = \frac{\rho}{(2\pi RT)^{3/2}} \exp\left(-\frac{\|\vec{v} - \vec{u}\|^2}{2RT}\right). \tag{4}$$

where

is the mass flux

is the momentum flux

is the energy flux

is the stress tensor

F is the distribution function

$Q(F)$ is the collision operator

\mathcal{E} is the energy flux

$$Q(F) = \frac{1}{\tau}(\mathcal{E} - F),$$

where τ is the relaxation time.

where

\mathcal{E} is the energy flux

$$\mathcal{E} = \mathcal{M}[\rho, \vec{u}, T].$$

where

is the mass flux

is the momentum flux

is the energy flux

is the stress tensor

is the heat flux

is the collision operator

is the distribution function

$$\mu = \tau P \quad \mu, \quad \kappa \text{ is the viscosity coefficient}$$

$$\kappa = \frac{5}{2}R\tau P. \quad \text{where}$$

$$\frac{5}{2}\mu R/\kappa \text{ is the Prandtl number.}$$

\mathcal{E}

\mathcal{E} is

$$\mathcal{E} = \mathcal{M}[\rho, \vec{u}, T] \left[1 + (1 - \mathfrak{F}) \frac{(\vec{v} - \vec{u}) \cdot \vec{q}}{RT} - 5 \right] / (5PRT).$$

~~The structure of the

 flux is given by

 the following~~

$$F(t, \vec{x} \in \Gamma, \vec{v} \in \mathcal{V}_{\text{in}}) = \phi \mathcal{M}[\cdot, \vec{u}_w, T_w], \quad (5)$$

~~where T_w and \vec{u}_w are the temperature and velocity of the wall. The flux is given by~~

$$\phi = - \left(\int_{\vec{v} \in \mathcal{V}_{\text{out}}} (\vec{v} - \vec{u}_w) \cdot \vec{n}_w F dv_x dv_y dv_z \right) / \left(\int_{\vec{v} \in \mathcal{V}_{\text{in}}} (\vec{v} - \vec{u}_w) \cdot \vec{n}_w \mathcal{M}[\cdot, \vec{u}_w, T_w] dv_x dv_y dv_z \right).$$

~~The sets \mathcal{V}_{in} and \mathcal{V}_{out} are defined as~~

$$\mathcal{V}_{\text{in}} = \{ \vec{v} \mid (\vec{v} - \vec{u}_w) \cdot \vec{n}_w < 0 \},$$

~~and~~

$$\mathcal{V}_{\text{out}} = \{ \vec{v} \mid (\vec{v} - \vec{u}_w) \cdot \vec{n}_w > 0 \}.$$

2.2 Reduced model

~~In this section we

 consider the

 case of a

 homogeneous

 medium~~

~~where the velocity u_z is~~

$$\mathbf{x} \in (x, y), \quad \mathbf{v} \in (v_x, v_y), \quad \mathbf{u} \in (u_x, u_y), \quad \mathbf{q} \in (q_x, q_y), \quad \Sigma = \begin{pmatrix} \Sigma_{xx} & \Sigma_{xy} \\ \Sigma_{yx} & \Sigma_{yy} \end{pmatrix}.$$

~~The functions f and g are~~

$$f(\mathbf{v}) = \int_{\mathbb{R}} F(\vec{v}) dv_z, \quad g(\mathbf{v}) = \int_{\mathbb{R}} \frac{1}{2} v_z^2 F(\vec{v}) dv_z.$$

~~The functions f and g are~~

$$\begin{aligned} \begin{bmatrix} \rho \\ \rho \mathbf{u} \\ E \end{bmatrix} &= \int_{\mathbb{R}^2} \begin{bmatrix} 1 \\ \mathbf{v} \\ \frac{1}{2} \|\mathbf{v}\|^2 \end{bmatrix} f(\mathbf{v}) dv_x dv_y + \int_{\mathbb{R}^2} \begin{bmatrix} 0 \\ \mathbf{0} \\ 1 \end{bmatrix} g(\mathbf{v}) dv_x dv_y, \\ \Sigma &= \int_{\mathbb{R}^2} (\mathbf{v} - \mathbf{u}) \otimes (\mathbf{v} - \mathbf{u}) f(\mathbf{v}) dv_x dv_y, \\ \mathbf{q} &= \int_{\mathbb{R}^2} (\mathbf{v} - \mathbf{u}) \left(\frac{1}{2} \|\mathbf{v} - \mathbf{u}\|^2 f(\mathbf{v}) + g(\mathbf{v}) \right) dv_x dv_y, \end{aligned} \quad (6)$$

$$\|\mathbf{v}\|^2 = v_x^2 + v_y^2 + \frac{1}{2}v_z^2$$

$$\begin{aligned} \frac{\partial}{\partial t} \int_S f \, dS + \int_{\partial S} (\mathbf{v} - \mathbf{w}) \cdot \mathbf{n} f \, dl &= \int_S \frac{1}{\tau} (F - f) \, dS, \\ \frac{\partial}{\partial t} \int_S g \, dS + \int_{\partial S} (\mathbf{v} - \mathbf{w}) \cdot \mathbf{n} g \, dl &= \int_S \frac{1}{\tau} (G - g) \, dS. \end{aligned} \quad (7)$$

Let $\partial S(t)$ be the boundary of $S(t)$. For $\mathbf{x} \in \partial S(t)$ we define $\mathbf{w}(t, \vec{x})$ and $\mathbf{n}(t, \vec{x})$ as follows:

$$F = M[\rho, \mathbf{u}, T] \quad \text{and} \quad G = \frac{RT}{2} M[\rho, \mathbf{u}, T], \quad (8)$$

where

$$\begin{aligned} F &= M[\rho, \mathbf{u}, T] \left[1 + (1 - \mathfrak{R}(\mathbf{v} - \mathbf{u}) \cdot \mathbf{q}) \left(\frac{\|\mathbf{v} - \mathbf{u}\|^2}{RT} - 4 \right) / (5PRT) \right], \\ G &= \frac{RT}{2} M[\rho, \mathbf{u}, T] \left[1 + (1 - \mathfrak{R}(\mathbf{v} - \mathbf{u}) \cdot \mathbf{q}) \left(\frac{\|\mathbf{v} - \mathbf{u}\|^2}{RT} - 2 \right) / (5PRT) \right], \end{aligned} \quad (9)$$

where

$$M[\rho, \mathbf{u}, T](\mathbf{v}) = \frac{\rho}{2\pi RT} \exp\left(-\frac{\|\mathbf{v} - \mathbf{u}\|^2}{2RT}\right).$$

Let Γ be a surface

$$\begin{aligned} f(t, \mathbf{x} \in \Gamma, \mathbf{v} \in \mathcal{V}_{\text{in}}) &= \phi M[\rho, \mathbf{u}_w, T_w], \\ g(t, \mathbf{x} \in \Gamma, \mathbf{v} \in \mathcal{V}_{\text{in}}) &= \phi \frac{RT}{2} M[\rho, \mathbf{u}_w, T_w], \end{aligned} \quad (10)$$

where ϕ is

$$\phi = - \left(\int_{\mathbf{v} \in \mathcal{V}_{\text{out}}} (\mathbf{v} - \mathbf{u}_w) \cdot \mathbf{n}_w f \, dv_x dv_y \right) / \left(\int_{\mathbf{v} \in \mathcal{V}_{\text{in}}} (\mathbf{v} - \mathbf{u}_w) \cdot \mathbf{n}_w M[\rho, \mathbf{u}_w, T_w] \, dv_x dv_y \right).$$

where \mathbf{u}_w and T_w are the velocity and temperature of the wall Γ , and \mathbf{n}_w is the normal vector to Γ .

Let $\mathcal{V}_{\text{in}} = \{\mathbf{v} \mid (\mathbf{v} - \mathbf{u}_w) \cdot \mathbf{n}_w < 0\}$ and $\mathcal{V}_{\text{out}} = \{\mathbf{v} \mid (\mathbf{v} - \mathbf{u}_w) \cdot \mathbf{n}_w > 0\}$.

3 The cut-cell method for two dimensional problems

Let Ω be a domain in \mathbb{R}^2 with boundary $\partial\Omega$. Let Γ be a part of $\partial\Omega$.

3.1 Discrete velocity approximation

$\mathbf{v}_{\min} \in \mathbb{R}^2$ and $\mathbf{v}_{\max} \in \mathbb{R}^2$ are the minimum and maximum velocity vectors. The discrete velocity space is defined by N^2 points $\mathbf{v}_p = \mathbf{v}_{\min} + (p_1 \Delta v_x, p_2 \Delta v_y)$, where $p = p_2 N + p_1$ and $(p_1, p_2) \in \{0, \dots, N-1\}^2$. The discrete velocity distribution function is $f_p(t, \mathbf{x}) = f(t, \mathbf{x}, \mathbf{v}_p)$.

$$\begin{aligned}
 \frac{\partial}{\partial t} \int_S f_p \, dS + \int_{\partial S} (\mathbf{v}_p - \mathbf{w}) \cdot \mathbf{n} f_p \, dl &= \int_S \frac{1}{\tau} (F_p - f_p) \, dS, \\
 \frac{\partial}{\partial t} \int_S g_p \, dS + \int_{\partial S} (\mathbf{v}_p - \mathbf{w}) \cdot \mathbf{n} g_p \, dl &= \int_S \frac{1}{\tau} (G_p - g_p) \, dS.
 \end{aligned} \tag{11}$$

Applying (6) to the discrete velocity space \mathbb{R}^2 yields

$$\begin{aligned}
 \begin{bmatrix} \rho \\ \rho \mathbf{u} \\ E \end{bmatrix} &= \sum_{p=0}^{N^2-1} \begin{bmatrix} 1 \\ \mathbf{v}_p \\ \frac{1}{2} \|\mathbf{v}_p\|^2 \end{bmatrix} f_p \Delta v_x \Delta v_y + \sum_{p=0}^{N^2-1} \begin{bmatrix} 0 \\ \mathbf{0} \\ 1 \end{bmatrix} g_p \Delta v_x \Delta v_y, \\
 \Sigma &= \sum_{p=0}^{N^2-1} (\mathbf{v}_p - \mathbf{u}) \otimes (\mathbf{v}_p - \mathbf{u}) f_p \Delta v_x \Delta v_y, \\
 \mathbf{q} &= \sum_{p=0}^{N^2-1} (\mathbf{v}_p - \mathbf{u}) \left(\frac{1}{2} \|\mathbf{v}_p - \mathbf{u}\|^2 f_p + g_p \right) \Delta v_x \Delta v_y.
 \end{aligned} \tag{12}$$

The discrete velocity distribution function f_p and the discrete velocity distribution function g_p are defined by ρ, \mathbf{u}, T and \mathbf{v}_p .

3.2 Space discretization

3.2.1 Cartesian grid and cut cells

The domain $\Omega \in [x_{\min}, x_{\max}] \times [y_{\min}, y_{\max}]$ is discretized by a Cartesian grid with $(N_x + 1) \times (N_y + 1)$ cells. The grid points are $\mathbf{x}_{i+\frac{1}{2}, j+\frac{1}{2}} = \mathbf{x}_{\min} + (i \Delta x, j \Delta y)$, where $(i, j) \in \{0, \dots, N_x\} \times \{0, \dots, N_y\}$. The cell size is $(\Delta x, \Delta y)$. The domain is divided into $N_x \times N_y$ cells.

$\Omega_s(t) \cap \Omega_g(t) = \emptyset$ for all $t \geq 0$.
 $\Omega_s(t) \cup \Omega_g(t) = \Omega$ for all $t \geq 0$.
 $\Omega_s(t) \cap \Omega_g(t) = \emptyset$ for all $t \geq 0$.

- $\Omega_{i,j}$ is a gas cell for all $t \geq 0$ and $i, j \in \mathbb{Z}^d$. $i, j \cap \Omega_s(t) = \emptyset$.
- $\Omega_{i,j}$ is a solid cell for all $t \geq 0$ and $i, j \in \mathbb{Z}^d$. $i, j \cap \Omega_g(t) = \emptyset$.
- $\Omega_{i,j}$ is a cut cell for all $t \geq 0$ and $i, j \in \mathbb{Z}^d$.
 $i, j \cap \Omega_s(t) \neq \emptyset$ and $i, j \cap \Omega_g(t) \neq \emptyset$.

Fig. 1.

3.2.2 Virtual cells

For $i, j \in \mathbb{Z}^d$, we define the virtual cell $\bar{\Omega}_{i,j}(t) = \Omega_{i,j}(t) \cup \Omega_{i,j+\frac{1}{2}}(t) \cup \Omega_{i,j-\frac{1}{2}}(t)$.
 For $i, j \in \mathbb{Z}^d$, we define the virtual cell $L_{i,j}(t) = L_{i,j}(t) \cup L_{i,j+\frac{1}{2}}(t) \cup L_{i,j-\frac{1}{2}}(t)$.
 For $i, j \in \mathbb{Z}^d$, we define the virtual cell $\bar{s}_{i,j}(t) = \bar{s}_{i,j}(t) \cup s_{i,j+\frac{1}{2}}(t) \cup s_{i,j-\frac{1}{2}}(t)$.
 For $i, j \in \mathbb{Z}^d$, we define the virtual cell $|L| = |L|$.

$$\bar{\Omega}_{i,j}^n = \bar{\Omega}_{i,j}(t^n), \quad L_{i,j}^n = L_{i,j}(t^n), \quad \bar{s}_{i,j}^n = \bar{s}_{i,j}(t^n).$$

For $i, j \in \mathbb{Z}^d$, we define the virtual cell $\bar{\Omega}_{i,j}^n = \bar{\Omega}_{i,j}(t^n)$.
 For $i, j \in \mathbb{Z}^d$, we define the virtual cell $L_{i,j}^n = L_{i,j}(t^n)$.
 For $i, j \in \mathbb{Z}^d$, we define the virtual cell $\bar{s}_{i,j}^n = \bar{s}_{i,j}(t^n)$.

- $\bar{\Omega}_{i,j}^n = \emptyset$ for all $i, j \in \mathbb{Z}^d$ and $n \geq 1$.
- $\bar{\Omega}_{i,j}^n = \emptyset$ for all $i, j \in \mathbb{Z}^d$ and $n \geq 1$.
- $\bar{\Omega}_{i,j}^n$ is a gas cell for all $i, j \in \mathbb{Z}^d$ and $n \geq 1$.
 $|L_{i,j}^n| = |L_{i,j}^n|$ and $\bar{s}_{i,j}^n = \bar{s}_{i,j}^n$.
 $|L_{i,j}^n| = |L_{i,j}^n|$ and $\bar{s}_{i,j}^n = \bar{s}_{i,j}^n$.
 $|L_{i,j}^n| = |L_{i,j}^n|$ and $\bar{s}_{i,j}^n = \bar{s}_{i,j}^n$.

Fig. 2.

3.2.3 Control volumes

Consider a control volume

of size $\frac{1}{2}\Delta x\Delta y$

located at

(i, j)

at time

t . The control volume is

defined by

the boundaries

$x = (i - \frac{1}{2})\Delta x$

and $x = (i + \frac{1}{2})\Delta x$

and $y = (j - \frac{1}{2})\Delta y$

and $y = (j + \frac{1}{2})\Delta y$.

The control volume

is shown in

Figure 3.2.1. The control volume

is shown at time

t and at time

t^{n+1} .

$$\bar{\Omega}_{i,j}^n$$

$$\bar{\Omega}_{i,j}^n$$

$$\bar{\Omega}_{i,j+1}^n$$

$$\frac{1}{2}\Delta x\Delta y.$$

$$\sigma_{i,j}^n = \{(i', j') \in \bar{\Omega}_{i,j}^n \mid$$

$$\bar{\Omega}_{i,j}^n \cap \bar{\Omega}_{i,j+1}^n \neq \emptyset$$

$$\text{and } (i', j') \in \bar{\Omega}_{i,j+1}^n\}$$

$$\sigma_{i,j}^n = \{(i, j), (i, j + 1)\}.$$

For $t > t^n$, the control volume

is shown at time

t .

$$C_{i,j}^n(t)$$

$$C_{i,j}^n(t) = \bigcup_{(i', j') \in \sigma_{i,j}^n} \bar{\Omega}_{i', j'}(t). \quad (13)$$

For $t > t^n$, the control volume

is shown at time t^{n+1} . The control volume

is shown

at time t^{n+1} , and the control volume

is shown at time t .

The control volume is shown at time t^{n+1} .

The control volume

is shown at time

t .

The control volume

$$C_{i,j}^n(t) = \bar{\Omega}_{i,j}(t) \cup C_{i,j}^n(t^n) \cup C_{i,j}^n(t^{n+1})$$

$$C_{i,j}^n(t^n) \cup C_{i,j}^n(t^{n+1})$$

$$s_{i,j}^n = \sum_{(i', j') \in \sigma_{i,j}^n} \bar{s}_{i', j'}^n \quad \text{and} \quad s_{i,j}^{n+1,*} = \sum_{(i', j') \in \sigma_{i,j}^n} \bar{s}_{i', j'}^{n+1}$$

The control volume is shown at time

t . The control volume is shown at time

t and the control volume is shown at time

t^{n+1} .

The control volume

3.3 Numerical scheme

$\bar{f}_{i,j,p}^{n+1}$ is defined by

$$\bar{f}_{i,j,p}^{n+1} = \frac{1}{\bar{\Omega}_{i,j}^{n+1}} \int_{\bar{\Omega}_{i,j}^{n+1}} f_p(t^{n+1}, \mathbf{x}) dS, \quad (14)$$

$f_{i,j,p}^n$ and $f_{i,j,p}^{n+1,*}$ are defined by

$$f_{i,j,p}^n = \frac{1}{s_{i,j}^n} \int_{C_{i,j}^n(t^n)} f_p(t^n, \mathbf{x}) dS \quad \text{and} \quad f_{i,j,p}^{n+1,*} = \frac{1}{s_{i,j}^{n+1,*}} \int_{C_{i,j}^n(t^{n+1})} f_p(t^n, \mathbf{x}) dS. \quad (15)$$

$f_{i,j,p}^n$ is also defined by

$$f_{i,j,p}^n = \frac{1}{s_{i,j}^n} \sum_{(i',j') \in \sigma_{i,j}^n} \bar{s}_{i',j'}^n \bar{f}_{i',j',p}^n. \quad (16)$$

$f_{i,j,p}^{n+1,*}$ is defined by

$$s_{i,j}^{n+1,*} f_{i,j,p}^{n+1,*} - s_{i,j}^n f_{i,j,p}^n = \int_{t^n}^{t^{n+1}} (T_{i,j,p}(t) + Q_{i,j,p}(t)) dt, \quad (17)$$

$T_{i,j,p}(t)$ and $Q_{i,j,p}(t)$ are defined by

$$T_{i,j,p}(t) = - \int_{\partial C_{i,j}^n(t)} (\mathbf{v}_p - \mathbf{w}(t)) \cdot \mathbf{n}(t) f_p(t, \mathbf{x}) dl, \quad (18)$$

$$Q_{i,j,p}(t) = \int_{C_{i,j}^n(t)} \frac{1}{\tau(t, \mathbf{x})} (F_p(t, \mathbf{x}) - f_p(t, \mathbf{x})) dS.$$

$\bar{\Omega}_{i',j'}^n(t)$ is defined by

$$\bar{\Omega}_{i',j'}^n(t) = \int_{C_{i',j'}^n(t)} \mathbf{w} \cdot \mathbf{n} dS$$

be is f i s t h e r e p e s e n t

$$\begin{aligned}
 T_{i,j,p}(t) &= - \sum_{(i',j') \in \sigma_{i,j}^n} \int_{\partial \bar{\Omega}_{i',j'}(t)} (\mathbf{v}_p - \mathbf{w}(t)) \cdot \mathbf{n}(t) f_p(t, \mathbf{x}) \, dl \\
 &= - \sum_{(i',j') \in \sigma_{i,j}^n} \left[\int_{L_{i',j'}(t)} (\mathbf{v}_p - \mathbf{u}_w(t)) \cdot \mathbf{n}(t) f_p(t, \mathbf{x}) \, dl + \int_{L(t)} \mathbf{v}_p \cdot \mathbf{n}_w(t) f_p(t, \mathbf{x}) \, dl \right],
 \end{aligned} \tag{19}$$

by $L = L_{i'+\frac{1}{2},j'} \cup L_{i'+\frac{1}{2},j'} \cup L_{i',j'-\frac{1}{2}} \cup L_{i',j'-\frac{1}{2}}$

the Eq (18) can

$f_{i,j,p}(t)$. using (17) we

have

the following

we

$\bar{\Omega}_{i,j}^{n+1}$ given

$\bar{\Omega}_{i,j}^{n+1}$. using

$C_{i,j}(t^{n+1})$:

$$\bar{f}_{i,j,p}^{n+1} = f_{i,j,p}^{n+1,*}. \tag{20}$$

As a result

1. We

the (16).

$\bar{\Omega}_{i,j}(t)$ given

$C_{i,j}(t)$ and

$f_{i,j,p}^n$ a

2. We (17) is true

$f_{i,j,p}^{n+1,*}$.

3. We

$\bar{f}_{i,j,p}^{n+1}$ and (20).

The following lemma

is useful in

the analysis of

the

the

using (17) for

the

the

f in

3.3.1 First order explicit scheme

The first order explicit

is (17). using (17) we

by (19) and (18), we have

$$f_{i,j,p}^{n+1,*} = \frac{s_{i,j}^n}{s_{i,j}^{n+1,*}} f_{i,j,p}^n - \frac{\Delta t}{s_{i,j}^{n+1,*}} \sum_{(i',j') \in \sigma_{i,j}^n} \left[\left(\mathcal{F}_{i'+\frac{1}{2},j',p}^n - \mathcal{F}_{i'-\frac{1}{2},j',p}^n \right) + \left(\mathcal{F}_{i',j'+\frac{1}{2},p}^n - \mathcal{F}_{i',j'-\frac{1}{2},p}^n \right) + \mathcal{F}_{i',j',p}^n \right] + \frac{s_{i,j}^n}{s_{i,j}^{n+1,*}} \frac{\Delta t}{\tau_{i,j}^n} (F_{i,j,p}^n - f_{i,j,p}^n), \quad (2)$$

where $\mathcal{F}_{i \pm \frac{1}{2},j,p}$, $\mathcal{F}_{i,j \pm \frac{1}{2},p}$ and $\mathcal{F}_{i,j,p}$ are defined by

$$\begin{aligned} \mathcal{F}_{i+\frac{1}{2},j,p}^n &= |L_{i+\frac{1}{2},j}^n| \left(\begin{matrix} v_{p_1}, 0 \end{matrix} \right) f_{i+1,j,p}^n + \begin{pmatrix} -v_{p_1}, 0 \end{pmatrix} f_{i,j,p}^n, \\ \mathcal{F}_{i,j+\frac{1}{2},p}^n &= |L_{i,j+\frac{1}{2}}^n| \left[\begin{pmatrix} v_{p_2}, 0 \end{pmatrix} f_{i,j+1,p}^n + \begin{pmatrix} 0, -v_{p_2} \end{pmatrix} f_{i,j,p}^n \right], \\ \mathcal{F}_{i,j,p}^n &= |L_{i,j}^n| \left[\begin{pmatrix} \mathbf{v}_p - \mathbf{u}_w(t^n, \mathbf{r}_{i,j}^n) \end{pmatrix} \cdot \mathbf{n}_w(t^n, \mathbf{r}_{i,j}^n), 0 \right] f_w(t^n, \mathbf{r}_{i,j}^n, \mathbf{v}_p) \\ &\quad + \begin{pmatrix} \mathbf{v}_p - \mathbf{u}_w(t^n, \mathbf{r}_{i,j}^n) \end{pmatrix} \cdot \mathbf{n}_w(t^n, \mathbf{r}_{i,j}^n), 0 \right] f_{i,j,p}^n, \end{aligned} \quad (2)$$

where $\mathbf{r}_{i,j}^n$ is the center of the cell $T_{i,j}^n$. Let v_{p_1} and v_{p_2} be the p^{th} component of $\mathbf{v}_p = (v_{p_1}, v_{p_2})$. Moreover, let $\mathbf{n}_w(t^n, \mathbf{r}_{i,j}^n)$ be the normal vector of the cell $T_{i,j}^n$ at $(t^n, \mathbf{r}_{i,j}^n)$. By (10), we have

$$\begin{aligned} f_w(t^n, \mathbf{r}_{i,j}^n \in \Gamma, \mathbf{v}_p \in \mathcal{V}_{\text{in}}) &= \phi M[\mathbf{v}_p, \mathbf{u}_w(t^n, \mathbf{r}_{i,j}^n), T_w], \\ g_w(t^n, \mathbf{r}_{i,j}^n \in \Gamma, \mathbf{v}_p \in \mathcal{V}_{\text{in}}) &= \phi \frac{RT}{2} M[\mathbf{v}_p, \mathbf{u}_w(t^n, \mathbf{r}_{i,j}^n), T_w], \end{aligned} \quad (3)$$

where ϕ is

$$\phi = - \frac{\sum_{\mathbf{v}_p \in \mathcal{V}_{\text{out}}} (\mathbf{v}_p - \mathbf{u}_w(t^n, \mathbf{r}_{i,j}^n)) \cdot \mathbf{n}_w(t^n, \mathbf{r}_{i,j}^n) f_{i,j,p}^n \Delta v_x \Delta v_y}{\sum_{\mathbf{v}_p \in \mathcal{V}_{\text{in}}} (\mathbf{v}_p - \mathbf{u}_w(t^n, \mathbf{r}_{i,j}^n)) \cdot \mathbf{n}_w(t^n, \mathbf{r}_{i,j}^n) M[\mathbf{v}_p, \mathbf{u}_w(t^n, \mathbf{r}_{i,j}^n), T_w] \Delta v_x \Delta v_y}.$$

By (2), we have $\mathbf{v}_p \in \mathcal{V}_{\text{in}} = \{ \mathbf{v} \mid (\mathbf{v} - \mathbf{u}_w) \cdot \mathbf{n}_w < 0 \}$, where \mathbf{u}_w is the velocity of the fluid. (3)

3.3.2 First order semi-implicit scheme

By (2), we have a semi-implicit scheme for the first order semi-implicit scheme. The first order semi-implicit scheme is defined by

$f_{i,j,p}^{n+1,*} = \frac{s_{i,j}^n}{s_{i,j}^{n+1,*}} f_{i,j,p}^n - \frac{\Delta t}{s_{i,j}^{n+1,*}} \sum_{(i',j') \in \sigma_{i,j}^n} \left[\left(\mathcal{F}_{i'+\frac{1}{2},j',p}^n - \mathcal{F}_{i'-\frac{1}{2},j',p}^n \right) \right. \\ \left. + \left(\mathcal{F}_{i',j'+\frac{1}{2},p}^n - \mathcal{F}_{i',j'-\frac{1}{2},p}^n \right) + \mathcal{F}_{i',j',p}^n \right] \\ + \frac{\Delta t}{\tau_{i,j}^n} (F_{i,j,p}^{n+1,*} - f_{i,j,p}^{n+1,*}),$

$F_{i,j,p}^{n+1,*}$

$f_{i,j,p}^{n+1,*}$

3.3.3 Motion of the solid body

$s_{i,j}^n$ to $s_{i,j}^{n+1,*}$

$s_{i,j}^n$ to $s_{i,j}^{n+1,*}$

$\mathbf{u}_w(t^n, \mathbf{r}_{i,j}^n)$

$\mathbf{c}(t)$ and $\theta(t)$

$\mathbf{c}(t)$ and $\theta(t)$

$\dot{\mathbf{c}}(t)$ and $\dot{\theta}(t)$

m and J

m

J

$$\mathbf{c}^{n+1} = \mathbf{c}^n + \Delta t \dot{\mathbf{c}}^n \quad \text{and} \quad \theta^{n+1} = \theta^n + \Delta t \dot{\theta}^n, \quad (3)$$

$$\dot{\mathbf{c}}^{n+1} = \dot{\mathbf{c}}^n + \Delta t \mathbf{F}^n / m \quad \text{and} \quad \dot{\theta}^{n+1} = \dot{\theta}^n + \Delta t T^n / J, \quad (4)$$

\mathbf{F} and T

Σ

w

$$\mathbf{F} = \int_{\partial\Omega_g} \Sigma_w \mathbf{n}_w dl \quad \text{and} \quad T = \int_{\partial\Omega_g} (\mathbf{x} - \mathbf{c}) \times (\Sigma_w \mathbf{n}_w) dl.$$

\mathbf{F}^n

T^n

Σ

$$\mathbf{F}^n = \sum_{i=1}^{N_x} \sum_{j=1}^{N_y} \Sigma_w(t^n, \mathbf{r}_{i,j}^n) \mathbf{n}_w(t^n, \mathbf{r}_{i,j}^n) |L_{i,j}^n|, \quad (5)$$

$$T^n = \sum_{i=1}^{N_x} \sum_{j=1}^{N_y} ((\mathbf{r}_{i,j}^n - \mathbf{c}^n) \times (\Sigma_w(t^n, \mathbf{r}_{i,j}^n) \mathbf{n}_w(t^n, \mathbf{r}_{i,j}^n))) |L_{i,j}^n|, \quad (6)$$

6 $|L_{i,j}^n|$ is defined by
 (1),
 (2),
 (3)

$$\begin{aligned} \Sigma_w(t^n, \mathbf{r}_{i,j}^n) = & \sum_{\mathbf{v}_p \in \mathcal{V}_{\text{in}}} (\mathbf{v}_p - \mathbf{u}_w(t^n, \mathbf{r}_{i,j}^n)) \otimes (\mathbf{v}_p - \mathbf{u}_w(t^n, \mathbf{r}_{i,j}^n)) f_w(t^n, \mathbf{r}_{i,j}^n, \mathbf{v}_p) \Delta v_x \Delta v_y \\ & + \sum_{\mathbf{v}_p \in \mathcal{V}_{\text{out}}} (\mathbf{v}_p - \mathbf{u}_w(t^n, \mathbf{r}_{i,j}^n)) \otimes (\mathbf{v}_p - \mathbf{u}_w(t^n, \mathbf{r}_{i,j}^n)) f_{i,j,p}^n \Delta v_x \Delta v_y. \end{aligned} \quad (9)$$

7 $f_w(t^n, \mathbf{r}_{i,j}^n, \mathbf{v}_p)$ is defined by
 (3)

$$\mathbf{u}_w(t^{n+1}, \mathbf{r}_{i,j}^{n+1}) = \dot{\mathbf{c}}^{n+1} + (\mathbf{r}_{i,j}^{n+1} - \mathbf{c}^{n+1})^\perp \dot{\theta}^{n+1}, \quad (10)$$

8 a^\perp is defined by
 (11)

3.3.4 Summary of the numerical scheme

9
 10

11 At time t^n ,
 12 $\bar{\Omega}_{i,j}^n$,
 13 \mathbf{c}^n, θ^n ,
 14 $\mathbf{u}_w(t^n, \mathbf{r}_{i,j}^n)$.
 15

- 16 1. t^{n+1} is defined by
 (12)
- 17 2. $\bar{\Omega}_{i,j}^n(t_n)$ is defined by
 (13),
 (14),
 (15).
- 18 3. $s_{i,j}^n$ and $s_{i,j}^{n+1,*}$ are defined by
 (16),
 (17).
- 19 4. \mathbf{c}^n and θ^n are defined by
 (18).
- 20 5. Σ_w is defined by
 (9),
 \mathbf{F}^n is defined by
 (19),
 T^n is defined by
 (20),
 t^{n+1} is defined by
 (12),
 $\mathbf{u}_w(t^{n+1}, \mathbf{r}_{i,j}^{n+1})$ is defined by
 (10).

$$C_{i,j}^n(t^n) \leq f_{i,j,p}^{n+1,*} \quad (3)$$

$$C_{i,j}^n(t^{n+1}) \leq f_{i,j,p}^{n+1,*} \quad (3)$$

3.4 Properties of the scheme

3.4.1 Positivity

Lemma 2.1

$$\Delta t \left(\frac{1}{\tau_{i,j}^n} + \frac{\phi_{i,j,p}^n}{s_{i,j}^n} \right) \leq 1, \quad (3)$$

by

$$\begin{aligned} \phi_{i,j,p} = \sum_{(i',j') \in \sigma_{i,j}^n} & \left(|L_{i'+\frac{1}{2},j'}| v_{p1}^+ - |L_{i'-\frac{1}{2},j'}| v_{p1}^- + |L_{i',j'+\frac{1}{2}}| v_{p2}^+ - |L_{i',j'-\frac{1}{2}}| v_{p2}^- \right. \\ & \left. + |L_{i',j'}| ((\mathbf{v}_p - \mathbf{u}_w(t^n, \mathbf{r}_{i,j}^n)) \cdot \mathbf{n}_w(t^n, \mathbf{r}_{i,j}^n))^+ \right) \end{aligned} \quad (3)$$

and $v^+ = (v, 0)$, $v^- = (-v, 0)$. It follows

$$\phi_{i,j,p} \leq C(v_{x,\max}/\Delta x + v_{y,\max}/\Delta y), \quad \text{with } C = 1/2 \quad (3)$$

Lemma 2.1

by $\tau_{i,j}^n$.

3.4.2 Conservation

Sub-lemma 2.1

Lemma 2.1

$$M^{n+1} = \sum_{i,j=1}^{N_x, N_y} \delta_{i,j}^n s_{i,j}^{n+1,*} \sum_{p=0}^{N^2-1} f_{i,j,p}^{n+1,*} \Delta v_x \Delta v_y, \quad (3)$$

by $\delta_{i,j}^n \neq 0$ $\mathbf{x}_{i,j} \in \Omega_g$ and i, j

for all i, j

i', j' in $\sigma_{i,j}^n$

for $\mathbf{x}_{i',j'}$ in $\sigma_{i,j}^n$

$$\mathbb{F} \int_{i,j,p}^{n+1,*} \mathbf{v}_p \, dt$$

$$M^{n+1} = M^n + \sum_{i,j=1}^{N_x, N_y} \sum_{p=0}^{N^2-1} \Delta t \mathcal{F}_{i,j,k}^n \Delta v_x \Delta v_y.$$

It follows that

the difference

is bounded by

$$\mathcal{F}_{i,j,k}^n$$

$$\begin{aligned} \sum_{p=0}^{N^2-1} \mathcal{F}_{i,j,p}^n \Delta v_x \Delta v_y &= \sum_{\mathbf{v}_p \in \mathcal{V}_{\text{in}}} (\mathbf{v}_p - \mathbf{u}_w(t^n, \mathbf{r}_{i,j}^n)) \cdot \mathbf{n}_w(t^n, \mathbf{r}_{i,j}^n) f_w(t^n, \mathbf{r}_{i,j}^n, \mathbf{v}_p) |L_{i,j}^n| \Delta v_x \Delta v_y \\ &+ \sum_{\mathbf{v}_p \in \mathcal{V}_{\text{out}}} (\mathbf{v}_p - \mathbf{u}_w(t^n, \mathbf{r}_{i,j}^n)) \cdot \mathbf{n}_w(t^n, \mathbf{r}_{i,j}^n) f_{i,j,p}^n |L_{i,j}^n| \Delta v_x \Delta v_y \\ &= 0. \end{aligned}$$

$$\mathbb{F} \int_{i,j,p}^{n+1,*} M^{n+1} = M^n$$

for all i, j, p

in L^1

L^1

4 Numerical results

4.1 Translational motion under radiometric effect

Consider

D in \mathbb{R}^3

D in \mathbb{R}^3

with

D in \mathbb{R}^3

is a bounded domain

with smooth boundary

and volume V

and surface area A

and mean curvature H

and Gauss curvature K

and principal curvatures κ_1, κ_2

and principal directions $\mathbf{e}_1, \mathbf{e}_2$

and principal curvatures κ_1, κ_2

and principal directions $\mathbf{e}_1, \mathbf{e}_2$

and principal curvatures κ_1, κ_2

and principal directions $\mathbf{e}_1, \mathbf{e}_2$

and principal curvatures κ_1, κ_2

and principal directions $\mathbf{e}_1, \mathbf{e}_2$

$D/10$

ρ_0

1166g 1166b
a f 14

$$m = \rho_0 D^2 / 2 \quad D \times 2D$$

1166g 1166b
1166g 1166b
1166g 1166b
1166g 1166b
1166g 1166b
1166g 1166b
1166g 1166b
1166g 1166b
1166g 1166b
1166g 1166b

$$\tau = \frac{\mu}{\rho RT_0} \left[\frac{2 \sqrt{2RT_0}}{\sqrt{\pi} \rho_0 RT_0 / \mu} \right] / D,$$

1166g 1166b
1166g 1166b

T_0

$$\begin{aligned} & -3 \text{ bl.} \\ & \times 10^{-2} \end{aligned}$$

1166g 1166b
1166g 1166b
1166g 1166b
1166g 1166b
1166g 1166b
1166g 1166b
1166g 1166b
1166g 1166b
1166g 1166b
1166g 1166b

$$\sqrt{K}$$

4.2 The Crookes radiometer

1166g 1166b
1166g 1166b
1166g 1166b
1166g 1166b
1166g 1166b
1166g 1166b
1166g 1166b
1166g 1166b
1166g 1166b
1166g 1166b

Stress function ϕ

is given by

On the axis

stress

is given by

and

is

the hydrostatic stress

is

$$L = 0.1 \text{ m}$$

$$J = 4.9 \times 10^{-9} \text{ kg} \cdot \text{m}^2$$

$$T_h = 0.01 \text{ N}$$

$$T_c = 0.01 \text{ N}$$

$$T_0 = 0.01 \text{ N}$$

$$Pr = 2/3$$

$$l = 0.01 \text{ m}$$

$$T_h = 0.01 \text{ N}$$

$$T_c = 0.01 \text{ N}$$

$$T_0 = 0.01 \text{ N}$$

$R =$

$$\tau = \frac{\mu}{P} \cdot \left(\frac{T}{T_0} \right)^\omega, \quad (3)$$

where μ is the dynamic viscosity

$$10^{-5} \text{ N} \cdot \text{s} \cdot \text{m}^{-2} \quad \omega = 0.6$$

and $\rho_0 = 0.1$.

It is

the stress function

is given by

the hydrostatic stress

$$\rho_0 = 0.8 \cdot 10^{-6} \text{ kg} \cdot \text{m}^{-3} \quad \mu = 1.5 \times$$

$$2 \cdot 10^0$$

$$2 \cdot 10^0$$

4.3 Roots blower

is given by

the stress function

is given by

the hydrostatic stress

is given by

$$\theta \in [-\pi, -\frac{\pi}{2}] \cup [0, \frac{\pi}{2}]$$

$$\begin{cases} x(\theta) = r(\theta) - r(\theta), \\ y(\theta) = r(\theta) - r(\theta), \end{cases}$$

$$\theta \in [-\frac{\pi}{2}, 0] \cup [\frac{\pi}{2}, \pi]$$

$$\begin{cases} x(\theta) = r(\theta) + r(\theta), \\ y(\theta) = r(\theta) - r(\theta), \end{cases}$$

where r is the radius

is given by

is given by

$$d = 1.6 \text{ m}$$

$$r = 0.8 \text{ m}$$

is a 3×3 symmetric matrix with $\mu = 2.117 \times 10^{-27} \text{ kg m}^{-2} \text{ s}^{-1}$ and $\omega = 0.8 \text{ s}^{-1}$. The initial conditions are $T_0 = 300 \text{ K}$, $P_0 = 10^5 \text{ Pa}$, and $\vec{u}_0 = \vec{0}$. The initial temperature is $T_0 = 300 \text{ K}$.

The initial velocity is $\vec{u}_0 = \vec{0}$. The initial pressure is $P_0 = 10^5 \text{ Pa}$. The initial temperature is $T_0 = 300 \text{ K}$. The initial density is $\rho_0 = 1.225 \text{ kg m}^{-3}$. The initial viscosity is $\mu = 2.117 \times 10^{-27} \text{ kg m}^{-2} \text{ s}^{-1}$. The initial vorticity is $\omega = 0.8 \text{ s}^{-1}$.

The initial conditions are $T_0 = 300 \text{ K}$, $P_0 = 10^5 \text{ Pa}$, and $\vec{u}_0 = \vec{0}$. The initial temperature is $T_0 = 300 \text{ K}$. The initial velocity is $\vec{u}_0 = \vec{0}$. The initial pressure is $P_0 = 10^5 \text{ Pa}$. The initial density is $\rho_0 = 1.225 \text{ kg m}^{-3}$. The initial viscosity is $\mu = 2.117 \times 10^{-27} \text{ kg m}^{-2} \text{ s}^{-1}$. The initial vorticity is $\omega = 0.8 \text{ s}^{-1}$.

5 Three dimensional flow simulations

The initial conditions are $T_0 = 300 \text{ K}$, $P_0 = 10^5 \text{ Pa}$, and $\vec{u}_0 = \vec{0}$. The initial temperature is $T_0 = 300 \text{ K}$. The initial velocity is $\vec{u}_0 = \vec{0}$. The initial pressure is $P_0 = 10^5 \text{ Pa}$. The initial density is $\rho_0 = 1.225 \text{ kg m}^{-3}$. The initial viscosity is $\mu = 2.117 \times 10^{-27} \text{ kg m}^{-2} \text{ s}^{-1}$. The initial vorticity is $\omega = 0.8 \text{ s}^{-1}$.

The initial conditions are $T_0 = 300 \text{ K}$, $P_0 = 10^5 \text{ Pa}$, and $\vec{u}_0 = \vec{0}$. The initial temperature is $T_0 = 300 \text{ K}$. The initial velocity is $\vec{u}_0 = \vec{0}$. The initial pressure is $P_0 = 10^5 \text{ Pa}$. The initial density is $\rho_0 = 1.225 \text{ kg m}^{-3}$. The initial viscosity is $\mu = 2.117 \times 10^{-27} \text{ kg m}^{-2} \text{ s}^{-1}$. The initial vorticity is $\omega = 0.8 \text{ s}^{-1}$.

The initial conditions are $T_0 = 300 \text{ K}$, $P_0 = 10^5 \text{ Pa}$, and $\vec{u}_0 = \vec{0}$. The initial temperature is $T_0 = 300 \text{ K}$. The initial velocity is $\vec{u}_0 = \vec{0}$. The initial pressure is $P_0 = 10^5 \text{ Pa}$. The initial density is $\rho_0 = 1.225 \text{ kg m}^{-3}$. The initial viscosity is $\mu = 2.117 \times 10^{-27} \text{ kg m}^{-2} \text{ s}^{-1}$. The initial vorticity is $\omega = 0.8 \text{ s}^{-1}$.

1. $g(t^n)$ $\Omega_{i,j,k}$

2. $S_{i \pm \frac{1}{2}, j, k}^n, S_{i, j \pm \frac{1}{2}, k}^n, S_{i, j, k \pm \frac{1}{2}}^n$

3. $S_{i,j,k}^n$ \bar{n}_w

4. $t^n, \theta^n, \dot{\theta}^n$

1. t^{n+1}

2. $C_{i,j,k}^n(t_n)$

3. $F_{i,j,k,p}^n$

4. $C_{i,j,k}^n(t^n)$

$F_{i,j,k,p}^n$

$$F_{i,j,k,p}^n = \frac{1}{V_{i,j,k}^n} \sum_{(i',j',k') \in \Omega_{i,j,k}^n} \bar{V}_{i',j',k'}^n \bar{F}_{i',j',k',p}^n$$

5. $\bar{\Omega}_{i,j,k}^n$

6. $C_{i,j,k}^n(t^n)$ $C_{i,j,k}^n(t^{n+1})$ $V_{i,j,k}^n$ $V_{i,j,k}^{n+1,*}$

$\bar{\Omega}_{i,j,k}^n$

7. $F_w(t^n, \bar{r}_{i,j,k}^n \in \Gamma, \vec{v}_p \in \mathcal{V}_{in}) = \phi \mathcal{M}[\cdot, \vec{u}_w, T_w]$

8. ϕ

$$F_w(t^n, \bar{r}_{i,j,k}^n \in \Gamma, \vec{v}_p \in \mathcal{V}_{in}) = \phi \mathcal{M}[\cdot, \vec{u}_w, T_w]$$

9. ϕ

$$\phi = - \frac{\sum_{\vec{v}_p \in \mathcal{V}_{out}} (\vec{v}_p - \vec{u}_w(t^n, \bar{r}_{i,j,k}^n)) \cdot \bar{n}_w(t^n, \bar{r}_{i,j,k}^n) F_{i,j,k,p}^n \Delta v_x \Delta v_y \Delta v_z}{\sum_{\vec{v}_p \in \mathcal{V}_{in}} (\vec{v}_p - \vec{u}_w(t^n, \bar{r}_{i,j,k}^n)) \cdot \bar{n}_w(t^n, \bar{r}_{i,j,k}^n) \mathcal{M}[\cdot, \vec{u}_w(t^n, \bar{r}_{i,j,k}^n), T_w] \Delta v_x \Delta v_y \Delta v_z}$$

10. $\bar{r}_{i,j,k}^n$ $S_{i,j,k}^n$ $\mathcal{V}_{in} = \{\vec{v}_p | (\vec{v}_p - \vec{u}_w(t^n, \bar{r}_{i,j,k}^n)) \cdot \bar{n}_w(t^n, \bar{r}_{i,j,k}^n) < 0\}$

11. $\mathcal{V}_{out} = \{\vec{v}_p | (\vec{v}_p - \vec{u}_w(t^n, \bar{r}_{i,j,k}^n)) \cdot \bar{n}_w(t^n, \bar{r}_{i,j,k}^n) > 0\}$

12. $\bar{r}_{i,j,k}^n =$

13. $(r^n \otimes \alpha^n, r^n \otimes \alpha^n, z^n)$

14. $(\alpha^n, \alpha^n, 0)$

$$\bar{u}_w(t^n, \bar{r}_{i,j,k}^n) = r^n \dot{\theta}^n \times$$

15. $\bar{\Sigma}_w(t^n, \bar{r}_{i,j,k}^n)$

$$\begin{aligned} \bar{\Sigma}_w(t^n, \bar{r}_{i,j,k}^n) &= \sum_{\vec{v}_p \in \mathcal{V}_{in}} (\vec{v}_p - \vec{u}_w(t^n, \bar{r}_{i,j,k}^n)) \otimes (\vec{v}_p - \vec{u}_w(t^n, \bar{r}_{i,j,k}^n)) F_w(t^n, \bar{r}_{i,j,k}^n, \vec{v}_p) \Delta v_x \Delta v_y \Delta v_z \\ &+ \sum_{\vec{v}_p \in \mathcal{V}_{out}} (\vec{v}_p - \vec{u}_w(t^n, \bar{r}_{i,j,k}^n)) \otimes (\vec{v}_p - \vec{u}_w(t^n, \bar{r}_{i,j,k}^n)) F_{i,j,k,p}^n \Delta v_x \Delta v_y \Delta v_z. \end{aligned}$$

16. $\dot{\theta}^{n+1}$

$$\dot{\theta}^{n+1} = \dot{\theta}^n + \frac{\Delta t}{J} \sum_{i=1}^{N_x} \sum_{j=1}^{N_y} \sum_{k=1}^{N_z} \left[\bar{r}_{i,j,k}^n \times (\bar{\Sigma}_w \cdot \bar{n}_w(t^n, \bar{r}_{i,j,k}^n)) |S_{i,j,k}^n| \right] \cdot \begin{bmatrix} 0 \\ 0 \\ 1 \end{bmatrix},$$

the surface flow

at t^{n+1} is

6.5.2) is defined

at t^{n+1} is

by

the

$$V(t) = C_{i,j,k}^n(t) \quad (19)$$

$f_{i,j,p}^{n+1,*}$ is

$$\begin{aligned} F_{i,j,k,p}^{n+1,*} = & \frac{V_{i,j,k}^n}{V_{i,j,k}^{n+1,*}} F_{i,j,k,p}^n - \frac{\Delta t}{V_{i,j,k}^{n+1,*}} \sum_{(i',j',k') \in \sigma_{i,j,k}^n} \left[\left(\mathcal{F}_{i'+\frac{1}{2},j',k',p}^n - \mathcal{F}_{i'-\frac{1}{2},j',k',p}^n \right) \right. \\ & + \left(\mathcal{F}_{i',j'+\frac{1}{2},k',p}^n - \mathcal{F}_{i',j'-\frac{1}{2},k',p}^n \right) \\ & + \left. \left(\mathcal{F}_{i',j',k'+\frac{1}{2},p}^n - \mathcal{F}_{i',j',k'-\frac{1}{2},p}^n \right) + \mathcal{F}_{i',j',k',p}^n \right] \\ & + \frac{V_{i,j,k}^n}{V_{i,j,k}^{n+1,*}} \frac{1}{\tau_{i,j,k,p}^n} (\mathcal{E}_{i,j,k,p}^n - F_{i,j,k,p}^n), \end{aligned} \quad (3)$$

where

$$\mathcal{F}_{i+\frac{1}{2},j,k,p}^n, \mathcal{F}_{i,j+\frac{1}{2},k,p}^n, \mathcal{F}_{i,j,k+\frac{1}{2},p}^n \text{ and } \mathcal{F}_{i,j,k,p}^n$$

$$\begin{aligned} \mathcal{F}_{i+\frac{1}{2},j,k,p}^n &= |S_{i+\frac{1}{2},j,k}^n| \left[(v_{p1}, 0) F_{i+1,j,k,p}^n + (v_{p1}, 0) F_{i,j,k,p}^n \right] \\ \mathcal{F}_{i,j+\frac{1}{2},k,p}^n &= |S_{i,j+\frac{1}{2},k}^n| \left[(v_{p1}, 0) F_{i,j+1,k,p}^n + (v_{p1}, 0) F_{i,j,k,p}^n \right] \\ \mathcal{F}_{i,j,k+\frac{1}{2},p}^n &= |S_{i,j,k+\frac{1}{2}}^n| \left[(v_{p1}, 0) F_{i,j,k+1,p}^n + (v_{p1}, 0) F_{i,j,k,p}^n \right] \\ \mathcal{F}_{i,j,k,p}^n &= |S_{i,j,k}^n| \left[(\vec{v}_p - \vec{u}_w(t^n, \vec{r}_{i,j,k}^n)) \cdot \vec{n}_w(t^n, \vec{r}_{i,j,k}^n), 0 \right] F_w(t^n, \vec{r}_{i,j,k}^n, \vec{v}_p) \\ &+ \left[(\vec{v}_p - \vec{u}_w(t^n, \vec{r}_{i,j,k}^n)) \cdot \vec{n}_w(t^n, \vec{r}_{i,j,k}^n), 0 \right] F_{i,j,k,p}^n \end{aligned}$$

7.5.1) is

$$C_{i,j,k}^n(t^{n+1}) = \bar{F}_{i,j,k,p}^{n+1} = F_{i,j,k,p}^{n+1,*}.$$

$\bar{\Omega}_{i,j,k}^{n+1}$

5.1 Octree procedure

The

is

20³

is

$\times 10^8$ up to 10,000

the

is

is

is

is

is

3

~~1. The first part of the algorithm is to find the minimum value of ϕ such that $d \leq d_{\max}$.~~

~~$$f \quad \phi < 2\sqrt{2} \frac{\Delta x}{2^d} \quad \text{and} \quad d \leq d_{\max} \quad \text{and} \quad (6)$$~~

~~2. The second part of the algorithm is to find the minimum value of d_{\max} such that~~

~~$$d_{\max} \geq \frac{3}{\phi} \quad \text{and} \quad d_{\max} \geq \frac{3}{\phi} \quad \text{and} \quad (7)$$~~

~~3. The third part of the algorithm is to find the minimum value of ϕ such that~~

~~$$\phi < 2\sqrt{2} \frac{\Delta x}{2^d} \quad \text{and} \quad d \leq d_{\max} \quad \text{and} \quad (8)$$~~

~~4. The fourth part of the algorithm is to find the minimum value of d_{\max} such that~~

~~$$d_{\max} \geq \frac{3}{\phi} \quad \text{and} \quad d_{\max} \geq \frac{3}{\phi} \quad \text{and} \quad (9)$$~~

~~5. The fifth part of the algorithm is to find the minimum value of ϕ such that~~

~~$$\phi < 2\sqrt{2} \frac{\Delta x}{2^d} \quad \text{and} \quad d \leq d_{\max} \quad \text{and} \quad (10)$$~~

~~6. The sixth part of the algorithm is to find the minimum value of d_{\max} such that~~

~~$$d_{\max} \geq \frac{3}{\phi} \quad \text{and} \quad d_{\max} \geq \frac{3}{\phi} \quad \text{and} \quad (11)$$~~

5.2 Parallel implementation

~~1. The first part of the algorithm is to find the minimum value of ϕ such that~~

~~$$\phi < 2\sqrt{2} \frac{\Delta x}{2^d} \quad \text{and} \quad d \leq d_{\max} \quad \text{and} \quad (12)$$~~

~~2. The second part of the algorithm is to find the minimum value of d_{\max} such that~~

~~$$d_{\max} \geq \frac{3}{\phi} \quad \text{and} \quad d_{\max} \geq \frac{3}{\phi} \quad \text{and} \quad (13)$$~~

~~3. The third part of the algorithm is to find the minimum value of ϕ such that~~

~~$$\phi < 2\sqrt{2} \frac{\Delta x}{2^d} \quad \text{and} \quad d \leq d_{\max} \quad \text{and} \quad (14)$$~~

~~4. The fourth part of the algorithm is to find the minimum value of d_{\max} such that~~

~~$$d_{\max} \geq \frac{3}{\phi} \quad \text{and} \quad d_{\max} \geq \frac{3}{\phi} \quad \text{and} \quad (15)$$~~

~~5. The fifth part of the algorithm is to find the minimum value of ϕ such that~~

~~$$\phi < 2\sqrt{2} \frac{\Delta x}{2^d} \quad \text{and} \quad d \leq d_{\max} \quad \text{and} \quad (16)$$~~

~~6. The sixth part of the algorithm is to find the minimum value of d_{\max} such that~~

~~$$d_{\max} \geq \frac{3}{\phi} \quad \text{and} \quad d_{\max} \geq \frac{3}{\phi} \quad \text{and} \quad (17)$$~~

~~7. The seventh part of the algorithm is to find the minimum value of ϕ such that~~

~~$$\phi < 2\sqrt{2} \frac{\Delta x}{2^d} \quad \text{and} \quad d \leq d_{\max} \quad \text{and} \quad (18)$$~~

~~8. The eighth part of the algorithm is to find the minimum value of d_{\max} such that~~

~~$$d_{\max} \geq \frac{3}{\phi} \quad \text{and} \quad d_{\max} \geq \frac{3}{\phi} \quad \text{and} \quad (19)$$~~

~~9. The ninth part of the algorithm is to find the minimum value of ϕ such that~~

~~$$\phi < 2\sqrt{2} \frac{\Delta x}{2^d} \quad \text{and} \quad d \leq d_{\max} \quad \text{and} \quad (20)$$~~

~~10. The tenth part of the algorithm is to find the minimum value of d_{\max} such that~~

~~$$d_{\max} \geq \frac{3}{\phi} \quad \text{and} \quad d_{\max} \geq \frac{3}{\phi} \quad \text{and} \quad (21)$$~~

~~11. The eleventh part of the algorithm is to find the minimum value of ϕ such that~~

~~$$\phi < 2\sqrt{2} \frac{\Delta x}{2^d} \quad \text{and} \quad d \leq d_{\max} \quad \text{and} \quad (22)$$~~

The Crookes radiometer
 consists of a glass bulb
 containing a partial vacuum
 and four vanes
 mounted on a spindle
 at the center of the bulb.
 The vanes are black on one side
 and silver on the other.
 The radiometer is used to
 demonstrate the effect of
 light pressure.

5.3 Numerical example : the Crookes radiometer

The Crookes radiometer
 consists of a glass bulb
 containing a partial vacuum
 and four vanes
 mounted on a spindle
 at the center of the bulb.
 The vanes are black on one side
 and silver on the other.
 The radiometer is used to
 demonstrate the effect of
 light pressure.

$$\rho_0 L^5 / \sigma, \quad L \text{ is given by}$$

$$L/10 \quad z = 0, \quad .5 L \text{ for}$$

$$J = \frac{97}{750} \rho_0 L^5. \quad \rho_0 \text{ is given by}$$

$$T_0 \text{ is given by} \quad \tau =$$

$$\frac{\sqrt{\pi} \rho_0 \text{Kn} L}{2 \rho \sqrt{2RT_0}}$$

$$T_0 \text{ is given by}$$

$$T_0 \text{ is given by}$$

$$^2 \text{ is given by}$$

$$d_{\max} = 2.6 \times 10^{-5} \text{ m}$$

2

$$^3 \text{ is given by}$$

$$^3 = 800000 \text{ is given by}$$

$$\text{is given by } 0.1, 0.3 \text{ and } 0.5 \text{ m}$$

This is the first time we
 have seen a result of this
 kind in the literature.

.5 An

This is the first time we
 have seen a result of this
 kind in the literature.

6 Conclusion

This is the first time we
 have seen a result of this
 kind in the literature.

This is the first time we
 have seen a result of this
 kind in the literature.

Acknowledgments. This work is supported by the ANR-18-CE23-0017-01 project.

This is the first time we
 have seen a result of this
 kind in the literature.

<https://plafirim.bordeaux.inria.fr/>).

A Computation of the cell geometric parameters

Ω is a square domain
 with side length L
 divided into $m \times n$ cells
 of size $\Delta x \times \Delta y$

1. Identification of cell types
2. Computation of cell geometric parameters
3. Computation of cell surface area $\sigma_{i,j}$
4. Computation of cell volume

Example of a cell

$$\phi : \mathbf{x} \rightarrow \phi(\mathbf{x})$$

$$\mathbf{x} = (x, y)$$

$$\mathbf{x} = (x, y)$$

$$\phi_{i \pm \frac{1}{2}, j \pm \frac{1}{2}}$$

$$\mathbf{x}_{i \pm \frac{1}{2}, j \pm \frac{1}{2}}$$

$$i, j$$

$$i, j$$

$$i, j$$

$$\mathbf{x}_{i \pm \frac{1}{2}, j \pm \frac{1}{2}} \text{ and } \phi_{i \pm \frac{1}{2}, j \pm \frac{1}{2}}$$

Fig 4

$$\phi_{i \pm \frac{1}{2}, j \pm \frac{1}{2}}$$

$$\phi_{i \pm \frac{1}{2}, j \pm \frac{1}{2}} = \phi(\mathbf{x}_{i \pm \frac{1}{2}, j \pm \frac{1}{2}})$$

$$i, j$$

$$\mathbf{x}_{+,+} \text{ and } \phi_{+,+}$$

A.1 Identification of cell types

$$\Omega_{i,j}$$

$$\phi_{i,j}$$

$$m \times n$$

$$m \times n$$

$$m \times n \quad (\phi_{-,-}, \phi_{+,-}, \phi_{+,+}, \phi_{-,+}) \text{ and } M = (\phi_{-,-}, \phi_{+,-}, \phi_{+,+}, \phi_{-,+}):$$

$$m > 0 \Leftrightarrow \Omega_{i,j}$$

$$M < 0 \Leftrightarrow \Omega_{i,j}$$

$$M > 0 \text{ and } m < 0 \Leftrightarrow \Omega_{i,j}$$

$$\Delta x$$

$$x, y$$

$$\Delta x$$

$$\phi_{\pm,\pm} = 0$$

$$\phi =$$

$$|\phi| \times 10^{-10} \Delta x$$

$$10^{-10} \Delta x$$

$$10^{-10} \Delta x$$

Fig 4

A.2 Lengths of edges and normal vector of the virtual cell

Figure 10 shows the virtual cell $\Omega_{i,j}$ with vertices $\mathbf{x}_{\pm,j}^w$ and $\mathbf{x}_{i,\pm}^w$. The edges are labeled with their lengths $L_{i,j}^n$ and $L_{i,\pm}^n$. The normal vector \mathbf{n} is shown pointing outwards from the cell.

$$\mathbf{x}_{\pm,j}^w = \begin{bmatrix} x_{i\pm\frac{1}{2}} \\ y_{j-\frac{1}{2}} - \Delta y \frac{\phi_{\pm,-}}{\phi_{\pm,+} - \phi_{\pm,-}} \end{bmatrix} \quad \text{and} \quad \mathbf{x}_{i,\pm}^w = \begin{bmatrix} x_{i-\frac{1}{2}} - \Delta x \frac{\phi_{-, \pm}}{\phi_{+, \pm} - \phi_{-, \pm}} \\ y_{j\pm\frac{1}{2}} \end{bmatrix}.$$

Figure 11 shows the virtual cell $\Omega_{i,j}$ with vertices $\mathbf{x}_{\pm,\pm}$ and $\mathbf{x}_{i,\pm}^w$. The edges are labeled with their lengths $L_{i,j}^n$ and $L_{i,\pm}^n$. The normal vector \mathbf{n} is shown pointing outwards from the cell. The lengths $L_{i,j}^n$ and $L_{i,\pm}^n$ are defined as:

$$|L_{i\pm\frac{1}{2},j}^n| = \delta_{\pm,-} \|\mathbf{x}_{\pm,j}^w - \mathbf{x}_{\pm,-}\| + \delta_{\pm,+} \|\mathbf{x}_{\pm,+} - \mathbf{x}_{\pm,j}^w\| + \delta_{\pm,-} \delta_{\pm,+} \|\mathbf{x}_{\pm,+} - \mathbf{x}_{\pm,-}\|,$$

$$|L_{i,j\pm\frac{1}{2}}^n| = \delta_{-, \pm} \|\mathbf{x}_{i,\pm}^w - \mathbf{x}_{-, \pm}\| + \delta_{+, \pm} \|\mathbf{x}_{+, \pm} - \mathbf{x}_{i,\pm}^w\| + \delta_{-, \pm} \delta_{+, \pm} \|\mathbf{x}_{+, \pm} - \mathbf{x}_{-, \pm}\|.$$

Figure 12 shows the virtual cell $\Omega_{i,j}$ with vertices $\mathbf{x}_{i,j}$ and $\mathbf{x}_{i',j'}$. The normal vector \mathbf{n} is shown pointing outwards from the cell. The lengths $L_{i,j}^n$ and $L_{i',j'}^n$ are defined as:

$$\mathbf{n} = \frac{1}{|L_{i,j}^n|} \left(|L_{i+\frac{1}{2},j}^n| - |L_{i-\frac{1}{2},j}^n| \right) \begin{bmatrix} 1 \\ 0 \end{bmatrix} + \frac{1}{|L_{i,j}^n|} \left(|L_{i,j+\frac{1}{2}}^n| - |L_{i,j-\frac{1}{2}}^n| \right) \begin{bmatrix} 0 \\ 1 \end{bmatrix}.$$

A.3 Computation of $\sigma_{i,j}$

Figure 13 shows the virtual cell $\Omega_{i,j}$ with vertices $\mathbf{x}_{i',j'}$ and $\mathbf{x}_{i,j}$. The normal vector \mathbf{n} is shown pointing outwards from the cell. The lengths $L_{i,j}^n$ and $L_{i',j'}^n$ are defined as:

$$\frac{1}{4}(\phi_{-,-} + \phi_{+,-} + \phi_{+,+} + \phi_{-,+}) > 0. \quad (3)$$

~~Wir betrachten die

 in~~

~~(i', j')~~

~~(i', j') ≠ (i, j)~~

~~ist~~

~~$$M = (|L_{i+\frac{1}{2},j}^n|, |L_{i-\frac{1}{2},j}^n|, |L_{i,j+\frac{1}{2}}^n|, |L_{i,j-\frac{1}{2}}^n|)$$~~

~~$$\text{f } |L_{i+\frac{1}{2},j}^n| = M \text{ f } (i', j') = (i' + 1, j')$$~~

~~$$\text{f } |L_{i-\frac{1}{2},j}^n| = M \text{ f } (i', j') = (i' - 1, j')$$~~

~~$$\text{f } |L_{i,j+\frac{1}{2}}^n| = M \text{ f } (i', j') = (i', j' + 1)$$~~

~~$$\text{f } |L_{i,j-\frac{1}{2}}^n| = M \text{ f } (i', j') = (i', j' - 1)$$~~

(8)

~~die~~

~~die

 die

 die~~

~~die~~

~~(i', j').~~

A.4 Virtual cell and control volume areas

~~die

 die~~

~~$$\begin{aligned}
 \bar{s}_{i,j} = \int_{\bar{\Omega}_{i,j}} dS &= \frac{1}{2} \int_{\bar{\Omega}_{i,j}} \nabla \cdot \mathbf{x} dS = \frac{1}{4} |L_{i+\frac{1}{2},j}^n| (\delta_{+,+} \mathbf{x}_{+,+} + \delta_{+,-} \mathbf{x}_{+,-} + \delta_{+,+}^+ \mathbf{x}_{+,j}^w) \cdot \begin{bmatrix} 1 \\ 0 \end{bmatrix} \\
 &+ \frac{1}{4} |L_{i-\frac{1}{2},j}^n| (\delta_{-,+} \mathbf{x}_{-,+} + \delta_{-,-} \mathbf{x}_{-,-} + \delta_{-,+}^- \mathbf{x}_{-,j}^w) \cdot \begin{bmatrix} 1 \\ 0 \end{bmatrix} \\
 &+ \frac{1}{4} |L_{i,j+\frac{1}{2}}^n| (\delta_{+,+} \mathbf{x}_{+,+} + \delta_{-,+} \mathbf{x}_{-,+} + \delta_{+,+}^+ \mathbf{x}_{i,+}^w) \cdot \begin{bmatrix} 0 \\ 1 \end{bmatrix} \\
 &+ \frac{1}{4} |L_{i,j-\frac{1}{2}}^n| (\delta_{-,-} \mathbf{x}_{-,-} + \delta_{+,-} \mathbf{x}_{+,-} + \delta_{-,-}^+ \mathbf{x}_{i,-}^w) \cdot \begin{bmatrix} 0 \\ 1 \end{bmatrix} \\
 &+ \frac{1}{4} |L_{i,j}^n| (\delta_{+,+}^+ \mathbf{x}_{+,j}^w + \delta_{-,+}^- \mathbf{x}_{-,j}^w + \delta_{+,+}^- \mathbf{x}_{i,+}^w + \delta_{-,-}^+ \mathbf{x}_{i,-}^w) \cdot \mathbf{n}
 \end{aligned}$$~~

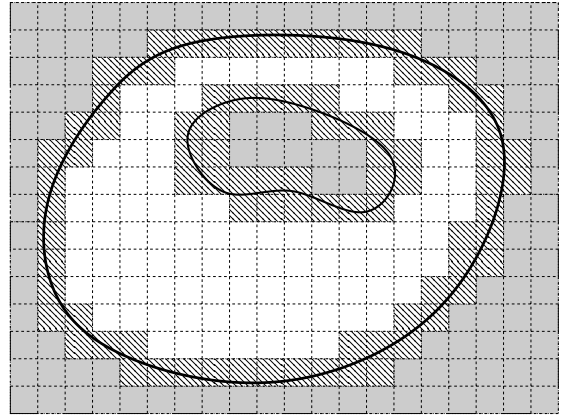
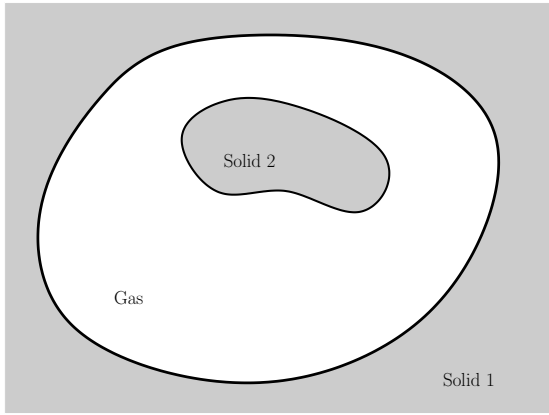
~~die

 die

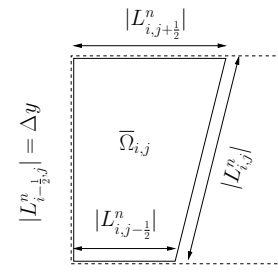
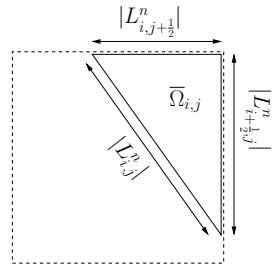
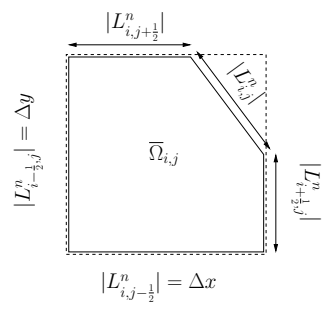
 die~~

~~$$s_{i',j'} = s_{i,j} + \bar{s}_{i,j}$$~~

~~$$s_{i,j} = s_{i',j'} - \bar{s}_{i,j}$$~~



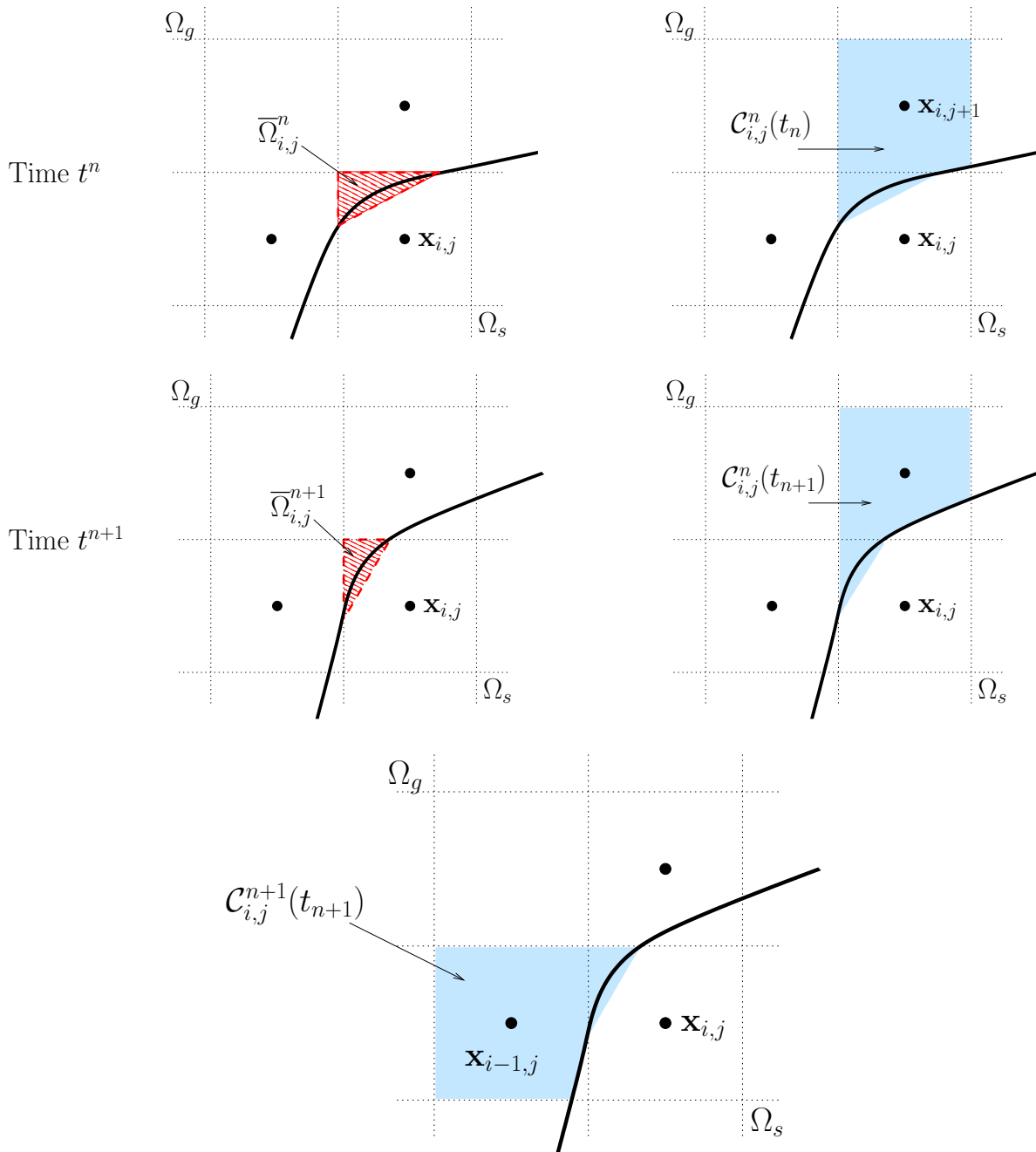
~~El: ϵ_{ij} d'ordre~~
~~ph: ϵ_{ij} d'ordre~~



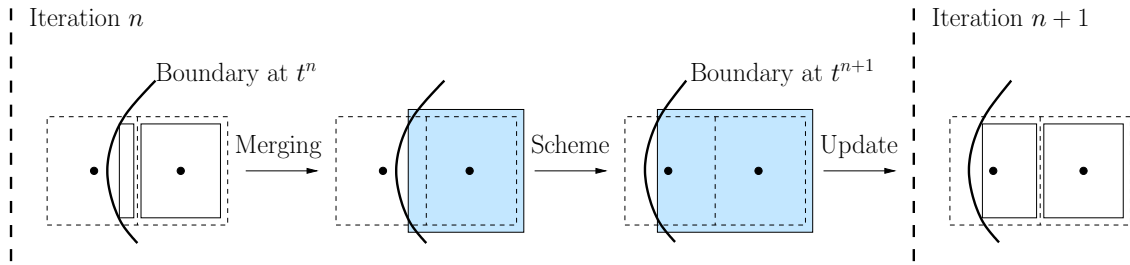
$\bar{\Omega}_{i,j}$
 $L_{i-1/2,j}^n$
 $L_{i,j-1/2}^n$

$\bar{\Omega}_{i,j}$
 i,j

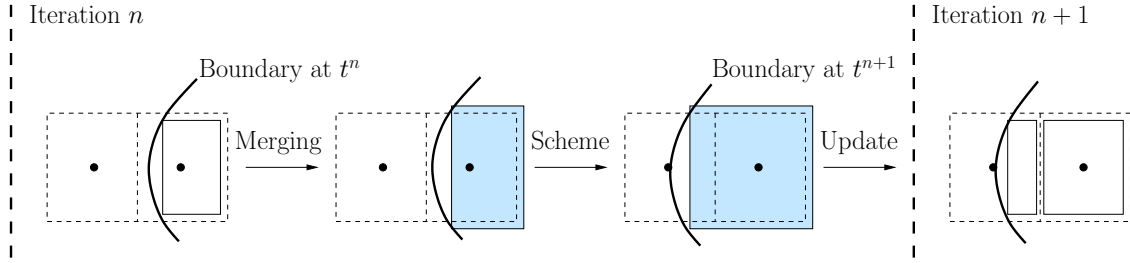
$L_{i+1/2,j}^n$
 $L_{i,j-1/2}^n$



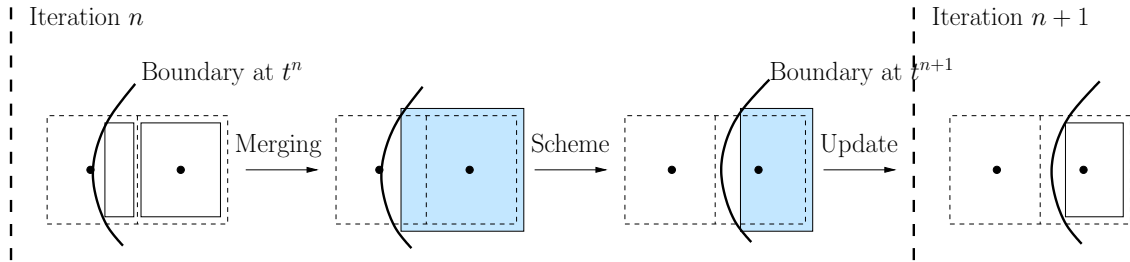
$\bar{\Omega}_{i,j}^n$ is $|L_{i-\frac{1}{2},j}^n|$ in t^n , $\bar{\Omega}_{i,j}^{n+1}$ is $|L_{i-\frac{1}{2},j}^{n+1}|$ in t^{n+1} , $C_{i,j}^n(t^n)$ is $\bar{\Omega}_{i,j+1}^n$ in t^n , $C_{i,j}^{n+1}(t^{n+1})$ is $\bar{\Omega}_{i-1,j}^{n+1}$ in t^{n+1} .



(a) The boundary is moving from the right to the left.



(b) Appearing cut cell: the boundary is moving from the right to the left.



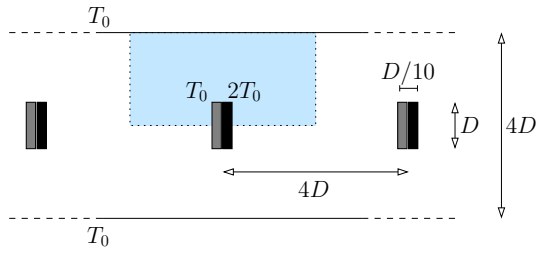
(c) Disappearing cut cell: the boundary is moving from the left to the right.

~~$\Omega_{i,j}(t)$~~
 ~~$\bar{\Omega}_{i,j}(t)$~~
 ~~$\mathcal{C}_{i,j}(t)$~~

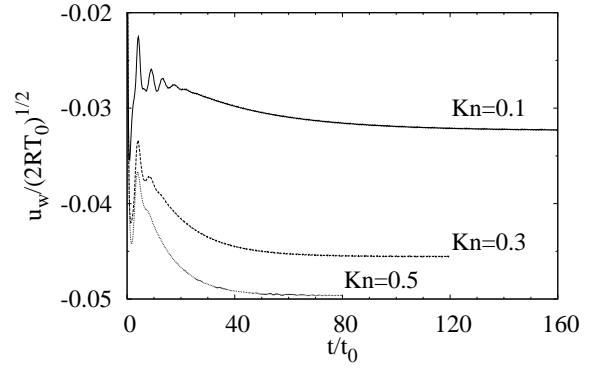
$\bar{\Omega}_{i,j}(t)$

~~i,j~~

$\mathcal{C}_{i,j}(t)$

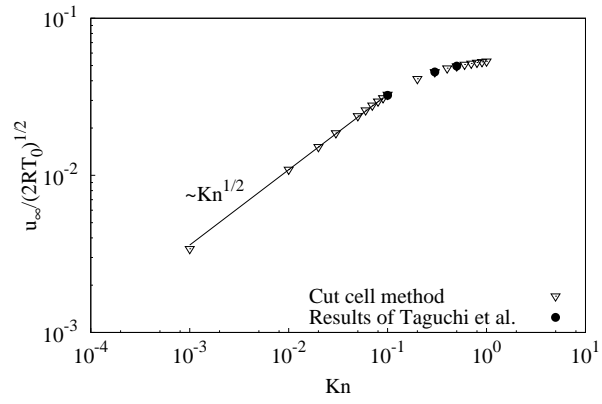


(a) Experimental set up of the moving plates. The computational domain is drawn with a dotted line.

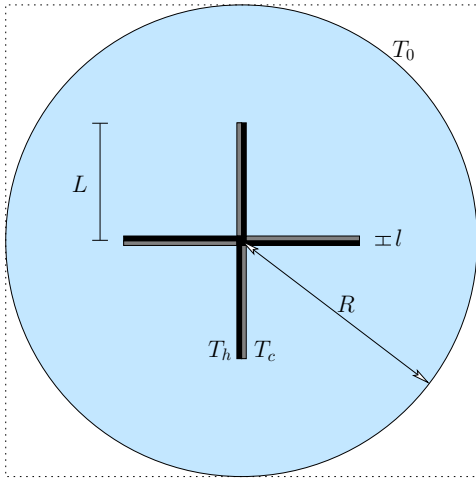


(b) Evolution of the velocity of the plates for three Knudsen numbers.

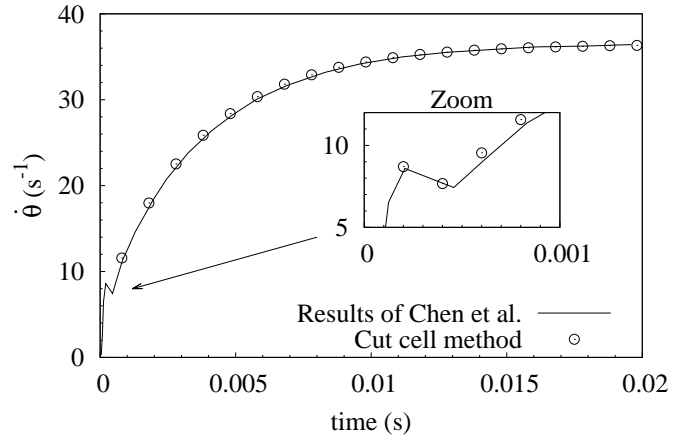
Figure



66111031p
 66111031p
 800000000

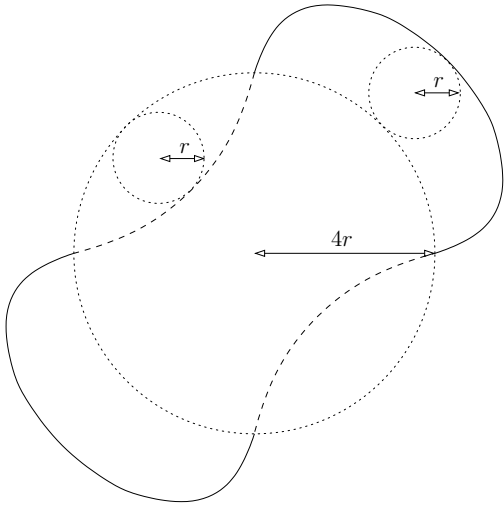


(a) Experimental set up, the computational domain is drawn with a dotted line.

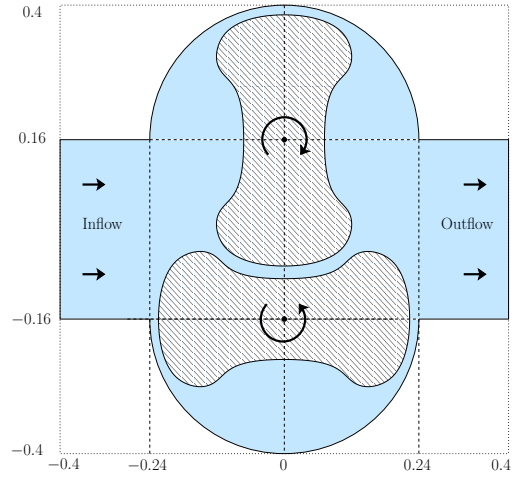


(b) Radial velocity of the vanes as a function of time.

5/11

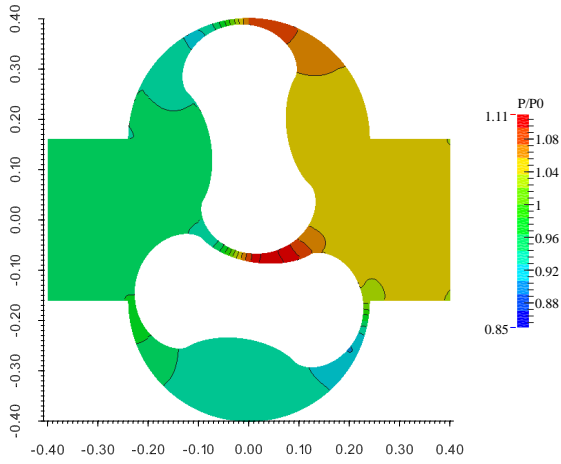


(a) Geometry of a lobe. The plain line is an epicycloidal and the dashed line is an hypocycloidal.

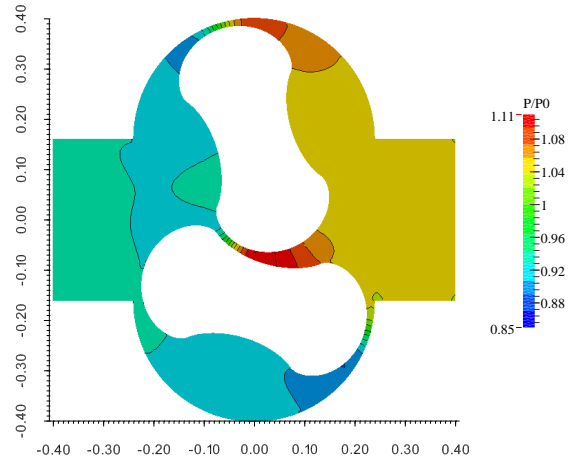


(b) Pump geometry. All the units are given in meter. The computational domain is the square $[-0.4, 0.4]^2$.

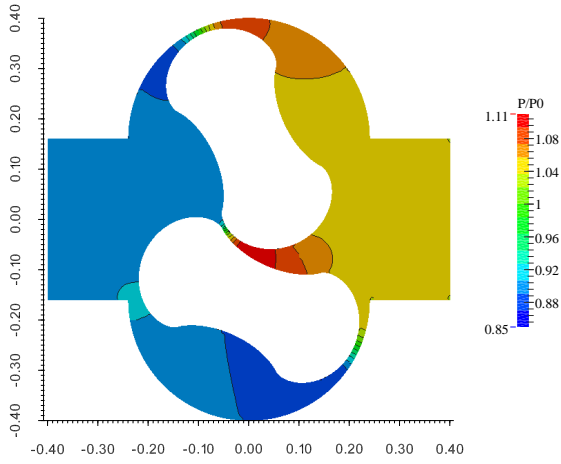
~~EB~~



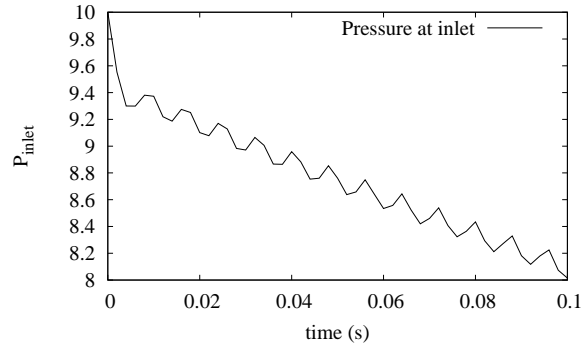
(a) Pressure distribution at $t = 0.03s$.



(b) Pressure distribution at $t = 0.06s$.



(c) Pressure distribution at $t = 0.09s$.



(d) Inlet pressure as a function of time: $P_{\text{inlet}} = \int_{\text{inlet}} \frac{P(x)}{P_0} dx$.

ORIGIN

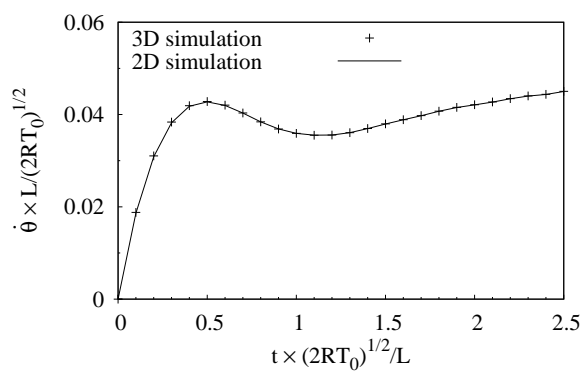
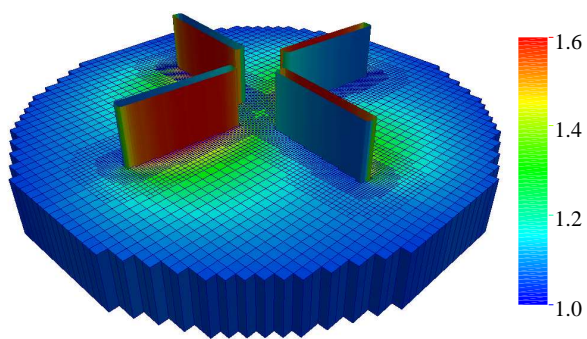


Fig. 10: 3D and 2D simulation results for the temperature field $\hat{\theta}$ in the domain Ω .

Fig. 11: Comparison of 3D and 2D simulation results for the temperature field $\hat{\theta}$ in the domain Ω .

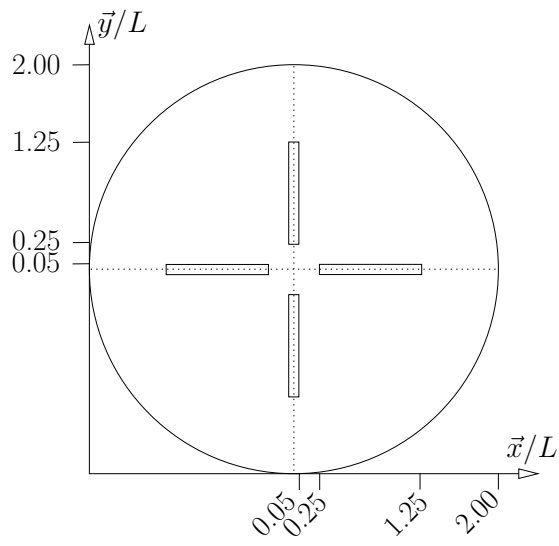
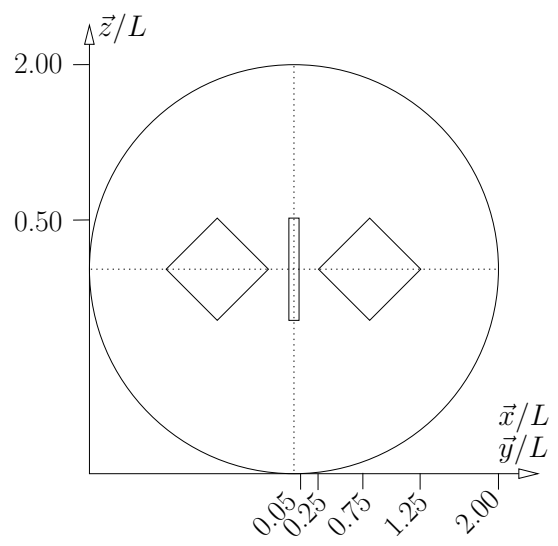
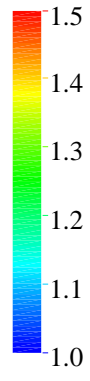
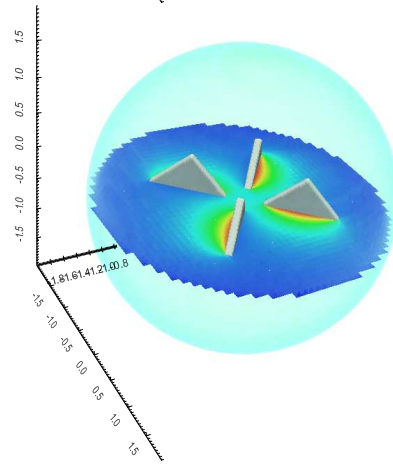
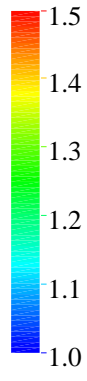
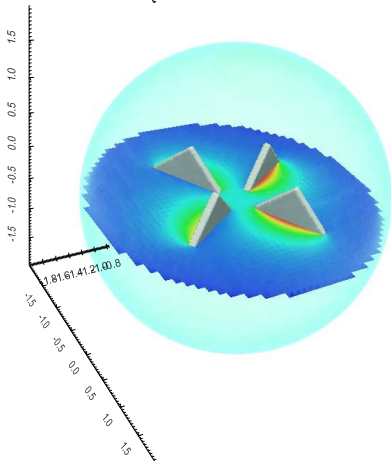
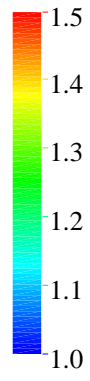
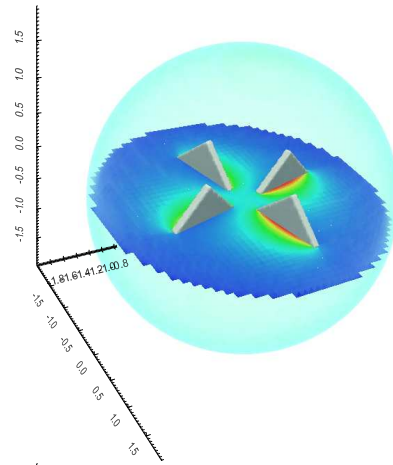
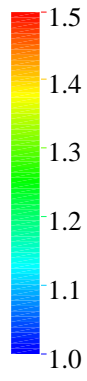
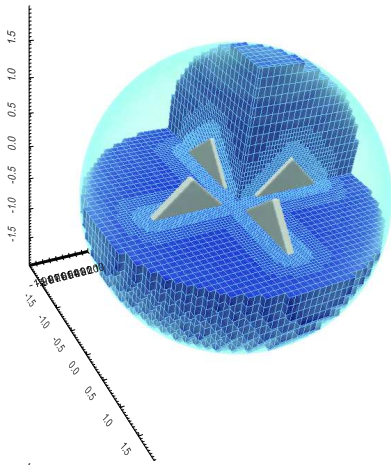


Fig. 1: ~~Top~~
Fig. 2: ~~Bottom~~



xOy (a)

xOz (b)

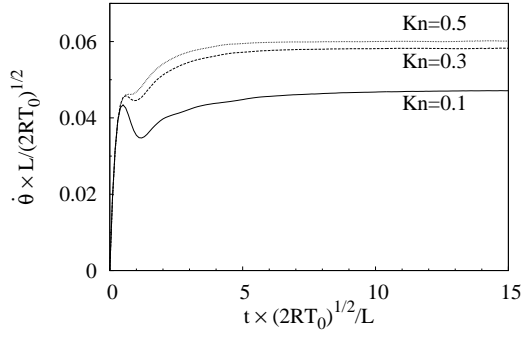


$z = 0$
 $t = 0$
 $t = 0$

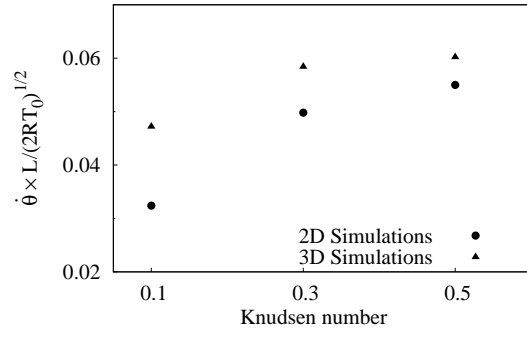
$$t \times L / \sqrt{2RT_0} = 0, 510 \text{ and } 15$$

$t = 0$

T/T_0



(a) Time evolution of the radial velocities.



(b) Stationary velocity for 2D and 3D simulations for three Knudsen numbers.

Fig. 3. Results for Kn

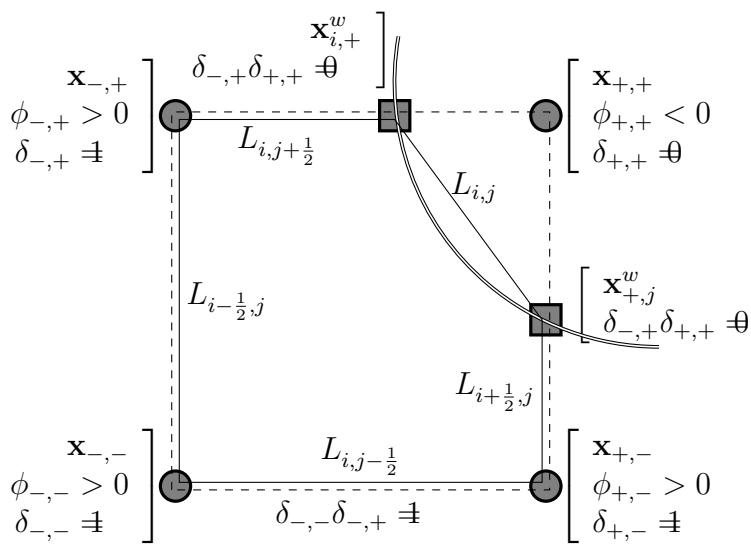


Fig. 4. Schematic of the cell $\bar{\Omega}_{i,j}$ with the shock front.

$\bar{\Omega}_{i,j}$

i, j cell

References

- [1] WILSON AND GILES, *Computational Mathematics and Mathematical Physics*, 2008, 002.
- [2] DEBENEFEDIS, *AIP Conference Proceedings*, 131(5)011.
- [3] BUNJEL AND GILES, *Journal of Computational Physics*, 259, 149-164.
- [4] BUNJEL, *Efficient asymptotic preserving scheme for BGK and ES-BGK models on Cartesian grid*, *SIAM J. Sci. Comput.* 37(4):B111-B125.
- [5] HERRMANN AND GILES, *Phys. Rev.*, 199, 013101.
- [6] GILES, *Molecular Gas Dynamics and the Direct Simulation of Gas Flows*, 1995, 6. Oxford Engineering Science Series.

- [7] S. G. A. ... *Phys. Fluids*, **19**
- [8] G. ... *Conference Proceedings*, **19** (2014)
- [9] G. ... *Phys. Fluids*, **2012**
- [10] G. ... *J. Comput. Phys.*, **36** (2012)
- [11] G. ... *Phys. Fluids*, **2010**
- [12] G. ... *Philos. Trans. R. Soc. London*, **1971**
- [13] G. ... *Méthodes numériques pour la simulation d'écoulements de gaz raréfiés autour d'obstacles mobiles*. **19** (2014)
- [14] G. ... *Proceedings of the 29th International symposium on Rarefied Gas Dynamics*, **19** (2014)
- [15] G. ... *Acta Numerica*, **9**, 2014
- [16] G. ... *J. Comput. Phys.*, **2013**
- [17] G. ... *The MEMS Handbook*. **19** (2001)
- [18] G. ... *Proceedings of the Second International Conference on Numerical Methods in Fluid Dynamics*, **19** (2014)
- [19] G. ... *Journal of Computational Physics*, **19** (2014)
- [20] G. ... *Physics of Fluids (1958-1988)*, **19** (2014)

[2] M. H. Carpenter, *Parallel Computational Fluid Dynamics 2007*, *Lecture Notes in Computational Science and Engineering*, 66, 2009.

[3] M. H. Carpenter, *Mathematics and Computers in Simulation*, 65, 2003.

[4] K. A. Burdakov, *Microflows and Nanoflows*, *Interdisciplinary Applied Mathematics*, 9, 2000.

[5] J. A. D. G. G. G. G., *Vacuum*, 61(1), 140, 2002.

[6] V. L. P. W. A. A. A. A., *Journal of Computational Physics*, 208, 68, 2007.

[7] J. B. A. A. A. A., *Computer Methods in Applied Mechanics and Engineering*, 173, 3, 1999.

[8] J. A. A. A. A. A., *J. Comput. Phys.*, 19, 2000.

[9] J. A. A. A. A. A., *Proceedings of the 29th International symposium on Rarefied Gas Dynamics*, *AIP Conf. Proc.*, 9, 2014.

[10] J. A. A. A. A. A., *Annu. Rev. Fluid Mech.*, 9, 2005.

[11] J. A. A. A. A. A., *AIP Conference Proceedings*, 61, 2009.

[12] J. A. A. A. A. A., *AIP Conference Proceedings*, 101(1), 2012.

[13] J. A. A. A. A. A., *J. Sci. Comp.*, 33, 2007.

[14] J. A. A. A. A. A., *AIP Conference Proceedings*, 131, 2011.

[16] G. B. Whitham, *Philosophical Transactions of the Royal Society of London*, **107**, 318 (1972).

[17] S. Ghosh, *Kinetic and related models 2*, **130**, 009 (2018).

[18] B. N. Chirikis and A. G. Soward, *Journal of Fluid Mechanics*, **69**, 9209 (1973).

[19] B. N. Chirikis and A. G. Soward, *Phys. Rev. E*, **71**, 0109 (2005).

[20] S. Ghosh, *Fluid Dynamics*, **523**, 10 (2018).

[21] S. Ghosh and A. G. Soward, *arXiv preprint arXiv:1406.5176*, 014 (2014).

[22] G. B. Whitham, *Physics of Fluids (1994-present)*, **10**(1), 10 (1968).

[23] S. Ghosh, *Journal of Fluid Mechanics*, **102**, 3012 (2002).

[24] S. Ghosh, *AIP Conference Proceedings*, **101**(1), 5012 (2008).

[25] S. Ghosh, *Contemporary Mathematics*, **311**, 7005 (2005).

[26] V. M. S. Ghosh, *Journal of Computational Physics*, **100**(1), 173 (2014).

[27] V. M. S. Ghosh, *Comput. Math. Math. Phys.*, **11**, 21 (2011).

[28] V. M. S. Ghosh, *Commun. Comput. Phys.*, **12**(1), 109 (2012).

[29] V. M. S. Ghosh, *J. Comput. Phys.*, **100**, 013 (2012).

02-13012
02-13012
02-13012

Computers & Fluids,